Appendices

Appendix 2.1

Additional Figures

FIGURE 1: Countries affected by blue water scarcity and stress

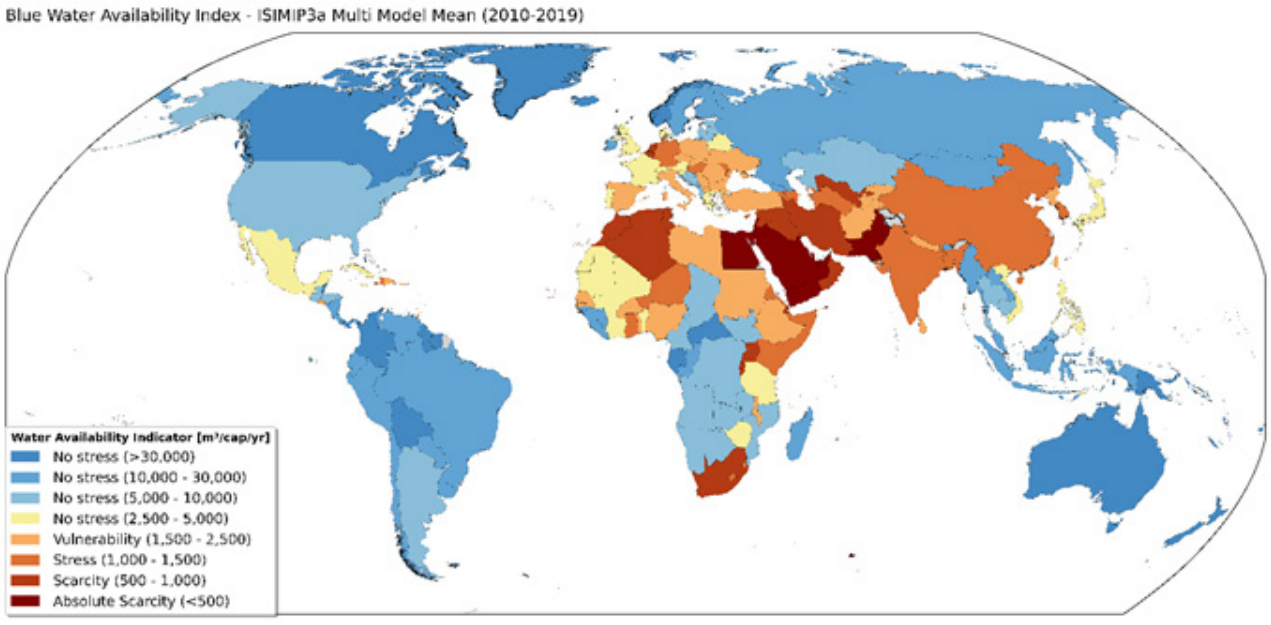

Figure 1: Blue water availability index aggregated to country scale averaged over the period 2010-2019 reported in m3/person/year– absolute scarcity <500; scarcity 500–1,000; stress 1,000–1,500; vulnerable 1,500–2,500 – or into "no stress" classes reflecting increasing blue water sufficiency: 2,500–5,000; 5,000–10,000; 10,000–30,000 and >30,000. Analysis is performed with total runoff output from the ISIMIP3a ensemble of global hydrological models (Frieler et al.; 2024)..

FIGURE 2: Countries affected by green water shortage

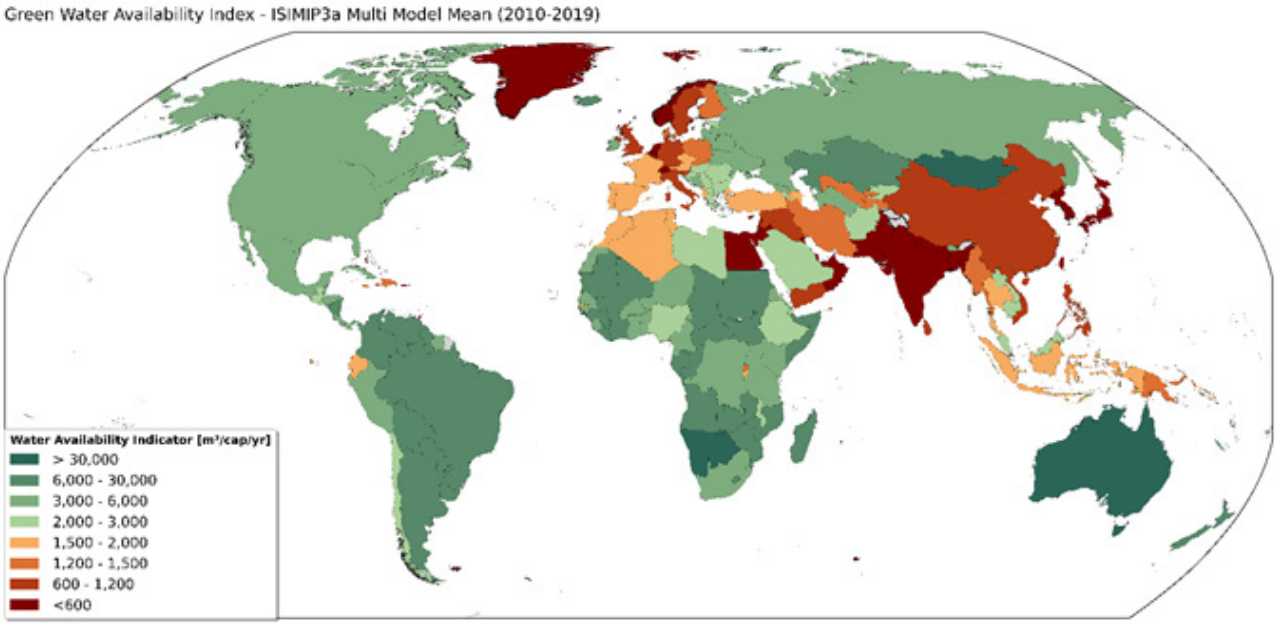

Figure 2: Green water availability index aggregated to country scale averaged over the period 2010-2019 reported in m3/person/year – green water shortage is <600 and green water sufficiency is >600, assuming various levels of transpiration efficiency that would be needed to produce an adequate standard diet, where 600 = 100% transpiration efficiency, 1,200 = 50%, 1,500 = 40%, 2,000 = 30%, 3,000 = 20%, 6,000 = 10%, and 30,000 = 2%. Analysis is performed with total runoff output from the ISIMIP3a ensemble of global hydrological models (Frieler et al.; 2024).

FIGURE 3: Countries classified by levels of combined blue and green water availability

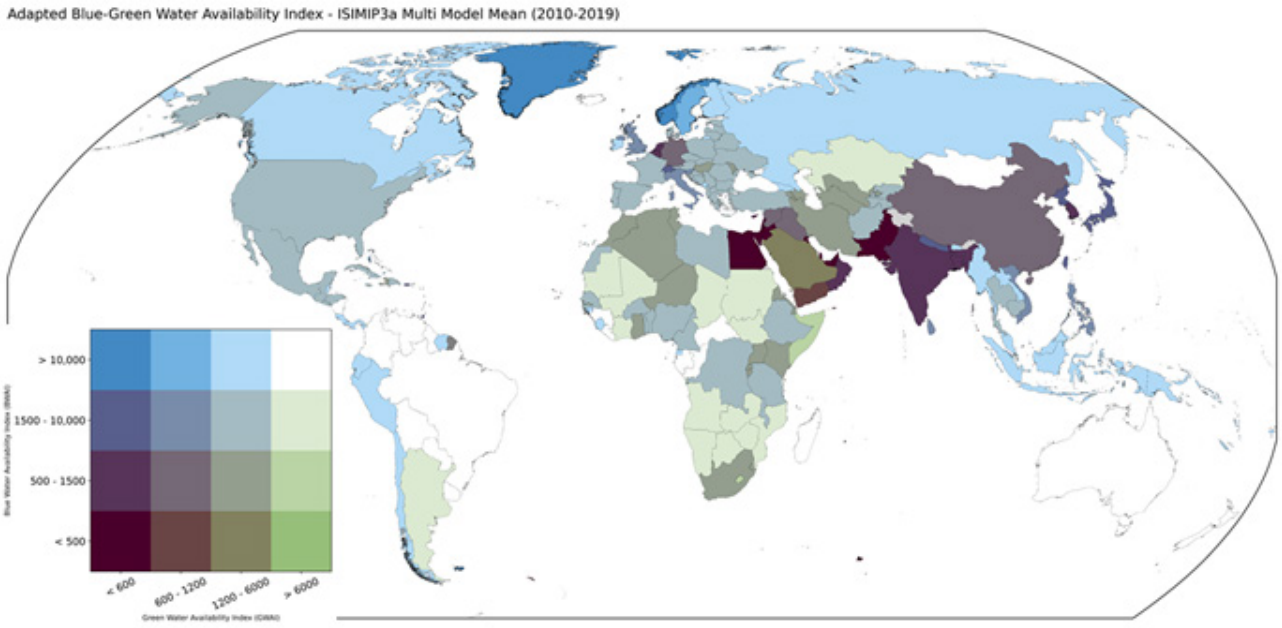

Figure 3: Combined green-blue water availability index aggregated to country scale averaged over the period 2010-2019 reported in m3/person/year. In the two-dimensional legend, blue water availability is depicted vertically and green water availability is depicted horizontally. Absolute green and blue water scarcity is indicated with dark purple in the lower left, green water sufficiency under blue water scarcity is green in the lower right, blue water sufficiency under green water shortage is blue in the upper left, and blue and green water sufficiency is white in the upper right. Analysis is performed with total runoff output from the ISIMIP3a ensemble of global hydrological models (Frieler et al.; 2024).

Methods

Water Availability Indices

- Blue water availability index (BWAI):

$$BWAI = \frac{BWA}{population} = \frac{Q_{tot} \times (1 - EFR)}{population}$$

, where *BWA* is blue water availability, Q_{tot} is total runoff and *EFR* is the environmental flow requirement (0.3).

TABLE 1: Blue Water Availability Classification

[m³/cap/year]	Classification
>30,000	No stress
10,000 – 30,000	No stress
5,000 – 10,000	No stress
2,500 – 5,000	No stress
1,500 – 2,500	Vulnerability
1,000 – 1,500	Stress
500 – 1,000	Scarcity
<500	Absolute scarcity

- Green water availability index (GWAI):

$$GWAI = \frac{GWA}{population} = \frac{ET_{agri} \times (1 - loss_{ET})}{population}$$

, where *GWA* is green water availability, ET_{agri} is evapotranspiration from rainfed cropland and permanent pasture, and $loss_{ET}$ is the fraction of *ET* that is lost before becoming available to plants (0.15).

TABLE 2: Green Water Scarcity Classification in terms of transpiration efficiency (TE) required to produce an adequate diet

[m³/cap/year]	Classification
>30,000	<2% TE
6,000 – 30,000	2-10% TE
3,000 – 6,000	10-20% TE
2,000 – 3,000	20-30% TE
1,500 – 2,000	30-40% TE
1,200 – 1,500	40-50% TE
600 – 1,200	50-100% TE
<600	Shortage

- Combined blue and green water assessment:

$$GBWAI = \frac{BWA + GWA}{population}$$

, where *GBWAI* stands for the combined Green – Blue Water Availability Indicator.

TABLE 3: Blue and green water availability classes for the combined water availability assessment

Blue water availability	Green water availability
[m³/cap/year]	[m³/cap/year]
>10,000	>6,000
1,500 – 10,000	1,200 – 6,000
500 – 1,500	600 – 1,200
<500	<600

FIGURE 4: Explanation of combined blue and green water availability classes

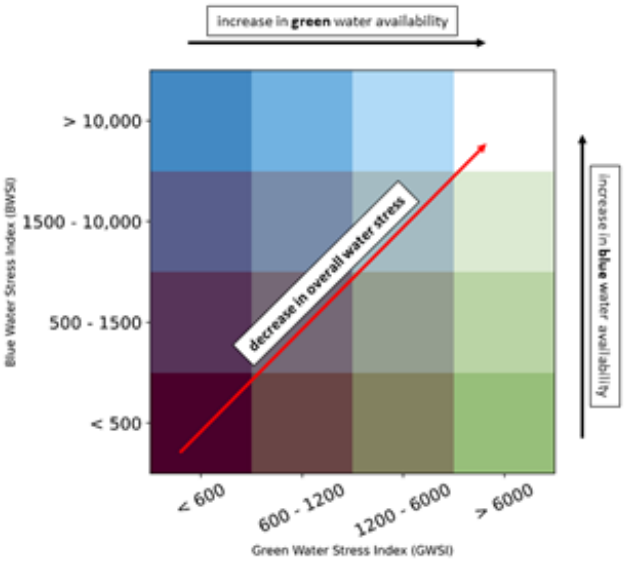

Atmospheric moisture flow analysis

- UTrack atmospheric moisture flow dataset

  —>Tuinenburg et al. (2020) and Tuinenburg and Staal (2020)

  —>Processing described in Tuinenburg et al. (2020), Fahrländer et al. (2024) and De Petrillo & Fahrländer et al. (in review 2024).

- Atmospheric moisture flow network between countries

  —> Network taken from De Petrillo & Fahrländer et al. (in review 2024).

Data

- ISIMIP3a (2010 – 2019)

  Data for the calculation of the water availability indices has been taken from the ISIMIP3a ensemble protocol (Frieler et al. 2024). The accessed data include a land-use classification to isolate evapotranspiration from agricultural lands, a country mask to aggregate the gridded data to country-scale, population data for the population-based water availability indices, as well as runoff (Qtot) for the blue water indicator and evapotranspiration (ET) for the green water indicator from a number of different hydrological models included in the ISIMIP3a protocol. The exact datasets of Qtot and ET are listed below.

Runoff (Q_{tot})	
Model	**Reference**
CLASSIC	Melton et al., 2020
CWatM	Burek et al., 2020
ELM-ECA	Zhu et al., 2019
H08	Hanasaki et al., 2017
HydroPy	Stacke & Stefan Hagemann et al., 2021
JULES-ES-VN6P3	Mathison et al., 2023
ORCHIDEE-MICT	Guimberteau et al., 2017
VISIT	Ito et al., 2018
WaterGAP2-2e	Müller Schmied et al., 2021

Evapotranspiration (ET)	
Model	**Reference**
CLASSIC	Melton et al., 2020
CWatM	Burek et. al., 2020
H08	Hanasaki et al., 2017
HydroPy	Stacke & Stefan Hagemann et al., 2021
JULES-ES-VN6P3	Mathison et al., 2023
MIROC-INTEG-LAND	Tokuta Yokohata et al., 2020
ORCHIDEE-MICT	Guimberteau et al., 2017
SSiB4-TRIFFID-Fire	Huang et al., 2020
VISIT	Ito et al., 2018
WaterGAP2-2e	Müller Schmied et al., 2021

References

R. Melton, Vivek K. Arora, Eduard Wisernig-Cojoc, Christian Seiler, Matthew Fortier, Ed Chan, and Lina Teckentrup et al. (2020). CLASSIC v1.0: the open-source community successor to the Canadian Land Surface Scheme (CLASS) and the Canadian Terrestrial Ecosystem Model (CTEM) – Part 1: Model framework and site-level performance. Geoscientific Model Development,13,2825–2850

Burek P, Satoh Y, Kahil T, Tang T, Greve P, Smilovic M, Guillaumot L, Zhao F, Wada Y et al. (2020). Development of the Community Water Model (CWatM v1.04) – a high-resolution hydrological model for global and regional assessment of integrated water resources management. Geoscientific Model Development,13,3267-3298

Zhu Q, Riley W, Tang J, Collier N, Hoffman F, Yang X, Bisht G et al. (2019). Representing Nitrogen, Phosphorus, and Carbon Interactions in the E3SM Land Model: Development and Global Benchmarking. Journal of Advances in Modeling Earth Systems,11,2238-2258

Hanasaki, N., Yoshikawa, S., Pokhrel, Y., Kanae, S. et al. (2017). A global hydrological simulation to specify the sources of water used by humans.

Tobias Stacke & Stefan Hagemann et al. (2021). HydroPy (v1.0): A new global hydrology model written in Python. Geosci. Model Dev.,14,7795–7816

Mathison, C., Burke, E., Hartley, A. J., Kelley, D. I., Burton, C., Robertson, E., Gedney, N., Williams, K., Wiltshire, A., Ellis, R. J., Sellar, A. A., and Jones, C. D. et al. (2023). Description and evaluation of the JULES-ES set-up for ISIMIP2b. Geoscientific Model Development,16,4249-4264

Tokuta Yokohata et al. (2020). MIROC-INTEG-LAND version 1: a global biogeochemical land surface model with human water management, crop growth, and land-use change. Geosci. Model Dev.,13,4713–4747

Guimberteau M, Zhu D, Maignan F, Huang Y, Yue C, Dantec-Nédélec S, Ottlé C, Jornet-Puig A, Bastos A, Laurent P, Goll D, Bowring S, Chang J, Guenet B, Tifafi M, Peng S, Krinner G, Ducharne A, Wang F, Wang T, Wang X, Wang Y, Yin Z, Lauerwald R, Joetzjer E, Qiu C, Kim H, Ciais P et al. (2017). ORCHIDEE-MICT (revision 4126), a land surface model for the high-latitudes: model description and validation. Geoscientific Model Development Discussions,None,1-65

Huang, H., Xue, Y., Li, F., and Liu, Y. et al. (2020). Modeling long-term fire impact on ecosystem characteristics and surface energy using a process-based vegetation–fire model SSiB4/TRIFFID-Fire v1.0. Geosci. Model Dev.,13,6029–6050

Ito, A. et al. (2018). Disequilibrium of terrestrial ecosystem CO2 budget caused by disturbance-induced emissions and non-CO2 carbon export flows: a global model assessment. Earth System Dynamics,10,685–709.

Müller Schmied, H., Trautmann, T., Ackermann, S., Cáceres, D., Flörke, M., Gerdener, H., Kynast, E., Peiris, T. A., Schiebener, L., Schumacher, M., and Döll, P. et al. (2021). The global water resources and use model WaterGAP v2.2e: description and evaluation of modifications and new features. Geosci. Model Dev. Discuss.

Tuinenburg, O. A., Theeuwen, J. J. E., & Staal, A. (2020). High-resolution global atmospheric moisture connections from evaporation to precipitation. *Earth System Science Data*, *12*(4), 3177–3188. https://doi.org/10.5194/essd-12-3177-2020

Tuinenburg, O. A., & Staal, A. (2020). Tracking the global flows of atmospheric moisture and associated uncertainties. *Hydrology and Earth System Sciences*, *24*(5), 2419–2435. https://doi.org/10.5194/hess-24-2419-2020

Rockström, J., Falkenmark, M., Karlberg, L., Hoff, H., Rost, S., & Gerten, D. (2009). Future water availability for global food production: The potential of green water for increasing resilience to global change. *Water Resources Research*, *45*(7). https://doi.org/10.1029/2007WR006767

Fahrländer, S. F., Wang Erlandsson, L., Pranindita, A., & Jaramillo, F. (2024). Hydroclimatic Vulnerability of Wetlands to Upwind Land Use Changes. *Earth's Future*, *12*(3). https://doi.org/10.1029/2023EF003837

Elena De Petrillo, Simon Fahrländer, Marta Tuninetti, Lauren Seaby Andersen, Luca Monaco, Luca Ridolfi, Francesco Laio. Reconciling tracked atmospheric water flows to close the global freshwater cycle, 29 April 2024, PREPRINT (Version 1) available at Research Square [https://doi.org/10.21203/rs.3.rs-4177311/v1]

Hersbach, H., Bell, B., Berrisford, P., Hirahara, S., Horányi, A., Muñoz Sabater, J., Nicolas, J., Peubey, C., Radu, R., Schepers, D., Simmons, A., Soci, C., Abdalla, S., Abellan, X., Balsamo, G., Bechtold, P., Biavati, G., Bidlot, J., Bonavita, M., … Thépaut, J. (2020). The ERA5 global reanalysis. *Quarterly Journal of the Royal Meteorological Society*, *146*(730), 1999–2049. https://doi.org/10.1002/qj.3803

European Commission Eurostat (ESTAT) GISCO. (2020). *Countries, 2020 - Administrative Units - Dataset ID 5C27B6C0-BC1C-4175-9B0B-783AEEBAAD61*. https://ec.europa.eu/eurostat/web/gisco/geodata/reference-data/administrative-unitsstatistical- units/countries

Jan Volkholz, Stefan Lange, Inga Sauer, Christian Otto (2024): ISIMIP3a population input data (v1.3). ISIMIP Repository. https://doi.org/10.48364/ISIMIP.822480.3

Porkka, M., Virkki, V., Wang-Erlandsson, L., Gerten, D., Gleeson, T., Mohan, C., Fetzer, I., Jaramillo, F., Staal, A., te Wierik, S., Tobian, A., van der Ent, R., Döll, P., Flörke, M., Gosling, S. N., Hanasaki, N., Satoh, Y., Müller Schmied, H., Wanders, N., … Kummu, M. (2024). Notable shifts beyond pre-industrial streamflow and soil moisture conditions transgress the planetary boundary for freshwater change. Nature Water, 2(3), 262–273. https://doi.org/10.1038/s44221-024-00208-7

Frieler, K., Volkholz, J., Lange, S., Schewe, J., Mengel, M., del Rocío Rivas López, M., Otto, C., Reyer, C. P. O., Karger, D. N., Malle, J. T., Treu, S., Menz, C., Blanchard, J. L., Harrison, C. S., Petrik, C. M., Eddy, T. D., Ortega-Cisneros, K., Novaglio, C., Rousseau, Y., … Bechtold, M. (2024). Scenario setup and forcing data for impact model evaluation and impact attribution within the third round of the Inter-Sectoral Impact Model Intercomparison Project (ISIMIP3a). *Geoscientific Model Development*, *17*(1), 1–51. https://doi.org/10.5194/gmd-17-1-2024

Appendix 3.1

Chapter 3 Appendixes

App 3.1 Data

Total water storage data

Estimates of changes in total terrestrial water storage (TWS) are obtained from the Gravity Recovery and Climate Experiment (GRACE) satellite mission. The GRACE satellite mission was launched in 2002 by the U.S. National Aeronautics and Space Administration (NASA) and the German Deutsche Forschungsanstalt für Luft und Raumfahrt (DLR) and extended in 2018 through a "follow-on" mission that is still ongoing. The satellites employed in the mission measure changes in the Earth's gravitational pull to elicit mass variations at all points on Earth. These mass variations uncovered by GRACE have been argued to be largely attributable to changes in water resources which move in large quantities and relatively fast across the Earth's surface.[1] The Goddard Flight Center (GSFC) mass concentration solution RL06v2.0 of GRACE is used, which reports monthly changes in the Earth's mass in centimetres of equivalent water height from 2003 to 2022 for 41,168 equal-area blocks, which measure 1° x 1° at the equator. Following previous studies, it is assumed that these mass changes reflect changes in total water storage (TWS), which encompasses groundwater, surface water, soil moisture, permafrost, snow, ice and biomass.[2] These medium-run trends undoubtedly cannot fully capture longer-run trends in water storage, and should therefore be interpreted cautiously. In particular, groundwater dynamics can be very slow-moving[3], implying that the insights gleaned from these two decades of observable data are not necessarily indicative of either early historical periods or the long-run future. However, they have been shown to be useful for characterising the sustainability of water resources[4], and provide valuable insights into social and economic vulnerabilities in the current moment, especially given the absence of longer time series of observations at the global scale.

The monthly data can be sourced from https://earth.gsfc.nasa.gov/geo/data/grace-mascons.

Groundwater depth and aridity data

To assess the combined risk from multiple water stress indicators, data on water table depth across the Earth is used.[5] The dataset combines government archives and published studies on 1,603,781 direct well measurements with a hydrological model to construct a continuous global map of groundwater depth at a 30 arc-seconds grid level. For the large majority (> 90%) of wells only one measurement over the period 2004 to 2014 is available, for the other sites where time series data exists the temporal mean is reported. The analysis is restricted to groundwater depth values deeper than 1mm, as shallower water tables indicate wetlands.

The cross-sectional data on annual mean water table depths used in this analysis is available at http://thredds-gfnl.usc.es/thredds/catalog/GLOBALWTDFTP/catalog.html.

The aridity indicator used in this study is derived from GSWP3-W5E5 historical climate data over the period 2003 to 2019. A monthly aridity indicator is calculated by dividing monthly total precipitation by monthly total evapotranspiration and indicates if evapotranspiration demand can

1 Byron D. Tapley et al., "GRACE Measurements of Mass Variability in the Earth System," Science, vol. 305, no. 5683, July 23, 2004, pp. 503–5, doi:10.1126/science.1099192.
2 M. Rodell et al., "Emerging Trends in Global Freshwater Availability," Nature, vol. 557, no. 7707, May 2018, pp. 651–59, doi:10.1038/s41586-018-0123-1.
3 J. Bredehoeft and T. Durbin, "Ground Water Development—The Time to Full Capture Problem," Groundwater 47, no. 4, 2009, pp. 506–14, doi:10.1111/j.1745-6584.2008.00538.x.
4 Johan Rockström et al., "Safe and Just Earth System Boundaries," Nature, vol. 619, no. 7968, July 2023, pp. 102–11, doi:10.1038/s41586-023-06083-8.
5 Y. Fan, H. Li, and G. Miguez-Macho, "Global Patterns of Groundwater Table Depth," Science, vol. 339, no. 6122, February 22, 2013, pp. 940–43, doi:10.1126/science.1229881.

be met by precipitation supply. For the purpose of this study, the average monthly aridity index between 2003 and 2019 is considered.

Historical weather data

Data on ambient temperature and precipitation for the period 2003 to 2022 is collected from the ERA5 Reanalysis product provided by the Copernicus Climate Change Service Climate Data Store. The reanalysis covers the period from 1940 to today and combines model as well as observational data to construct a consistent data-set with global coverage on a large number of land and oceanic climate variables. Data on ambient temperature 2m above the surface, total precipitation is available at an hourly resolution and at a 0.25°-by-0.25° grid. This high resolution data is aggregated to the GRACE grid using area weighting and calculated monthly average temperature in °C and monthly total precipitation in centimetres. The raw data can be obtained here:

https://cds.climate.copernicus.eu/cdsapp#!/dataset/reanalysis-era5-single-levels?tab=overview

Climate projections

Climate projections are collected from five global climate models (GCM) from the Coupled Model Intercomparison Project Phase 6 (CMIP6) under the intermediate emissions scenario RCP4.5. For the purpose of this study the following GCMs are considered, which span a wide range of equilibrium climate sensitivities (from 2.6°C to 5.3°C): GFDL-ESM4, IPS-CM6A-LR, MPI-ESM1-2-HR, MRI-ESM2-0, and UKESM1-0-LL. Data on average monthly temperature and total monthly precipitation from each of the global climate models is obtained for the period 2003 to 2050, where projections from 2003 to 2014 are retrospective. For each GCM, projections for the future period (2020 to 2050) are benchmarked against simulations from the same model for the baseline period (2003 to 2022) to account for time-invariant biases in local model projections.

Global atmospheric moisture flows (UTrack)

Global terrestrial-based atmospheric moisture flows, on a 1.0 degree resolution for both the source locations and downwind precipitation location, were obtained from the UTrack database.[6] Tracked atmospheric moisture flows over 2008-2017 were aggregated into a matrix of bilateral connections between sources and sinks using ERA5 reanalysis data at the monthly level. The dataset was generated using "UTrack", a Lagrangian moisture tracking model developed by Tuinenburg and Staal.[7] Using iterative simulations, numerous moisture particles were released at random locations and heights within each cell, and their movements were tracked based on wind speed and direction from ERA5 reanalysis data. At each time step, a portion of moisture particles within each cell are allocated to rainfall events. The tracked moisture particles at the end of the simulation are counted in each destination cell and allocated to source cells based on a tracking identifier, generating the cell-to-cell AMF matrix. The UTrack model was refined with detailed sensitivity analysis to test various assumptions and uncertainties affecting the accuracy of moisture tracking and hydrologically relevant statistics.

The dataset from Tuinenburg and Staal (2020) is available from the PANGAEA archive at https://doi.pangaea.de/10.1594/PANGAEA.912710.

Agriculture data

For our statistical analysis, data on physical areas under irrigated conditions, representing the area where crops are grown on land that is equipped for irrigation in hectares, from the Spatial Production Allocation model (SPAM) dataset is used. SPAM, developed by the International Food Policy Research Institute (IFPRI), is a hybrid cross-sectional product that integrates census, satellite and model data to provide global crop distribution estimates for 42 crops at a 5 arc-minutes resolution. The dataset distinguishes between irrigated and rainfed areas based on the Global Map of Irrigated Areas (GMIA v5), which includes the amount of area equipped for irrigation around the year 2005. Global crop statistics from SPAM are available at https://mapspam.info.

6 The model code can be obtained from: https://github.com/ObbeTuinenburg/UTrack-atmospheric-moisture

7 Tuinenburg, Obbe A. and Arie Staal. "Tracking the global flows of atmospheric moisture and associated uncertainties." Hydrol. Earth Syst. Sci., vol. 24, no. 5, 12 May. 2020, pp. 2419-35, doi:10.5194/hess-24-2419-2020.

Projections of future irrigation from 2020 to 2050 are constructed using the historical trend in irrigation. High resolution gridded data on area equipped for irrigation (AEI) for the years 2000, 2005, 2010 and 2015[8] and used to estimate linear trends through grid-specific regressions. These grid-cell specific linear trends are extrapolated for the future period (2020 to 2050) to obtain the total projected irrigated area over the period. Historical data on areas equipped for irrigation can be obtained from https://zenodo.org/records/7809342.

For the descriptive risk analysis, additional data on agricultural production, harvested area and potential yield under rainfed and irrigated conditions is collected from the Global Agro-Ecological Zones (GAEZ v4) dataset. The dataset is a hybrid product based on census and model data, offering gridded crop information at a high spatial resolution of 5 arcminutes for 26 different crops. Data on all cereals reported in the dataset is obtained to ensure comparability across units. Actual production and harvested area are based on aggregate national statistics from FAO statistics for the years 2009-2011 and downscaled to the individual spatial units. Agro-climatic potential yield is collected under high input levels and CRUTS32 historical climate over the period 1981 to 2012 and describes the yield potential of crops under given climatic, soil and terrain conditions. The GAEZ data can be sourced from https://gaez.fao.org.

Population data

Global population distribution data is acquired from the Global Human Settlements Layer (GHSL) database, developed by the European Commission. This dataset encompasses estimates of residential population derived from census and administrative units and further disaggregated to the grid cell level. The data is available at 5-year intervals, spanning the years 1975 to 2020, and further includes future projections for 2025 and 2030. For our analysis, data on the distribution of residential population for the year 2020 is used and obtained at the most detailed level of disaggregation available, which corresponds to a spatial resolution of 30 arcseconds. Population data from the GHSL can be retrieved from https://human-settlement.emergency.copernicus.eu/dataToolsOverview.php.

Human Development Index data

Global high resolution estimates of the United Nations Human Development Index (HDI) are obtained from the HDI estimates on a global 0.1 x 0.1 degree grid 2019 (v2) database.[9] Using a downscaling technique based on national and provincial administrative HDI data from 2018, daytime and nighttime satellite imagery and machine learning, this dataset provides HDI estimates at a 0.1 degree grid cell level. The disaggregated HDI estimates are available at https://www.mosaiks.org/hdi.

App 3.2 Methods

1. Risks to food security

To analyse future threats to agriculture arising from water stress, potential production losses if currently irrigated cropped land could no longer be irrigated are computed. The potential production loss for each grid cell () is defined as:

$$Loss_i = AreaIrr_i \; x \; (YieldIrr_i - YieldRain_i)$$

where is the area currently irrigated in 1000 hectares and and denote the potential yield under irrigated and rainfed conditions, respectively, in kg dry weight per hectare. Under the assumption that the impact of irrigation on potential yield is linearly separable from other factors affecting yield, the difference between potential yield under irrigated and rainfed conditions identifies the yield gain from irrigating in every location. Data on irrigated area and potential yield comes from GAEZ. Our analysis is restricted to wheat, rice, maize, sorghum, millet and barley since these crops are characterised by comparable units.

2. Drivers of changes in Total Water Storage

The effect of temperature and precipitation on changes in total water storage (TWS) in the long-run is identified using within grid-cell variation in temperature, precipitation and TWS.

8 Piyush Mehta et al., "Half of Twenty-First Century Global Irrigation Expansion Has Been in Water-Stressed Regions," Nature Water 2, no. 3, March 2024, pp. 254–61, doi:10.1038/s44221-024-00206-9.

9 Luke Sherman et al., "Global High-Resolution Estimates of the United Nations Human Development Index Using Satellite Imagery and Machine-Learning," Working Paper, Working Paper Series National Bureau of Economic Research, March 2023, doi:10.3386/w31044.

To model this relationship, consider the short run model:

$$(1)\ \Delta TWS_{im} = \beta^{SR} T_{im} + \gamma^{SR} P_{im} + FE + \varepsilon_{im},$$

where $\Delta TWS_{im} = TWS_{im} - TWS_{im-1}$ is the month-to-month change in total water storage from month $m-1$ to month m in grid cell i, T_{im} and P_{im} are the average temperature in °C and total precipitation in cm, respectively, in grid cell i in month m, FE represents grid-cell and basin-by-time period fixed effects, and ε_{im} denotes the idiosyncratic error term. This model has clear hydrologic grounding based on standard water balance where a change in water storage in a water system is equal to the difference between water inflow (precipitation) and outflow (evapotranspiration, net-runoff) during a time interval with temperature affecting TWS through crop water demand and evapotranspiration. While such a short-run model is informative for understanding vulnerability, it cannot shed light on longer-run dynamics that are critical for sustainability.

To model the long-run impact of temperature and precipitation on TWS, the short-run model is aggregated over 6-year time intervals, which gives the following final model:

$$(2)\ TWS_{iM} - TWS_{i0} = \beta^{LR} \sum_{m=1}^{M} T_{im} + \gamma^{LR} \sum_{m=1}^{M} P_{im} + FE + \varepsilon_{im},$$

where $TWS_{iM} - TWS_{i0}$ is the change in TWS over each 6-year time interval in the data and M is equal to 72 (6 years times 12 months). The grid-cell and basin-by-time period fixed effects control for all grid-cell specific time-invariant (e.g. soil, vegetation) and basin specific factors varying between the 6-year time intervals that affect TWS. The idiosyncratic error terms ε are clustered by basin allowing for correlation of model errors within basins (e.g. due to hydrological connectivity within basins). The coefficients of interest are β^{LR} and γ^{LR} representing the long-run monthly change in TWS for a persistent 1 unit shift in monthly temperature and precipitation, respectively, assuming that the 6-year window is sufficiently long to account for long-run re-equilibration effects. Only if the system adjusts immediately (i.e. there are no long-run re-equilibration effects) will the short-run and the long-run regression models (equation 1 and 2) recover the same β and γ in expectation.

As a capital investment, irrigation varies little over time and has longer-run impacts on TWS. To model the impact of irrigation on total water storage, the following cross-sectional model is employed:

$$(3)\ TWS_i^{trend} = \alpha_b + \delta I_i + \zeta W_i + \varepsilon_i,$$

where TWS_i^{trend} is the linear trend in total water storage (TWS) over the GRACE period (2003 - 2022) in grid cell i.[10] Basin fixed effects (α_b) control for time-invariant differences across basins that affect trends in TWS. Irrigated cropped area (fraction) in grid cell i is denoted by I_i, such that δ is the coefficient of interest representing the effect of irrigation (moving from no irrigation to full irrigation in a location) on the annual change in TWS. W_i denotes climate controls (anomalies in average yearly temperature and precipitation over the GRACE period from 2003 to 2022 relative to a 1980 to 2000 average baseline), that account for heterogeneity in temperature and precipitation trends across locations that could be correlated with the level of irrigation and would thus have confounding effects if omitted. The error term is denoted by ε and is clustered at the basin level.

Using the estimated temperature-TWS and precipitation-TWS relationship, $\widehat{\beta^{LR}}$ and $\widehat{\gamma^{LR}}$ estimated from model (2), historical and future counterfactual changes in TWS are calculated. To calculate the change in TWS attributable to past climatic changes, TWS changes over the GRACE period are compared to those that would have prevailed had the world experienced mid-20th century climatic conditions (i.e., the climate observed from 1951 to 1970) during this 2003-2022 period. In the future counterfactual simulation, TWS changes under mid century climatic conditions, projected by GCMs, are benchmarked against TWS changes under a stationary climate defined as that observed over the 2003-2022 GRACE record.

The total change in TWS in each grid cell i attributable to historical climatic changes is estimated as follows:

$$(4)\ \Delta TWS_i^{historical\ warming} = \widehat{\beta^{LR}} \left(\sum_{m=1}^{M} T_{im}^{2003-2022} - \sum_{m=1}^{M} T_{im}^{1951-1970} \right),$$

$$(5)\ \Delta TWS_i^{historical\ wetting/drying} = \widehat{\gamma^{LR}} \left(\sum_{m=1}^{M} P_{im}^{2003-2022} - \sum_{m=1}^{M} P_{im}^{1951-1970} \right),$$

10 Trends are estimated through grid-specific regressions with month fixed effects to remove the effects of seasonality.

$\Delta TWS_i^{historical\ warming}$ and $\Delta TWS_i^{historical\ wetting/drying}$ denote the total change in TWS over the 20 years of the GRACE record (2003-2022) attributable to warming and wetting/drying trends since 1951 to 1970. $T_{im}^{2003-2022}$ and $T_{im}^{1951-1970}$ are observed average temperature in grid cell i and month m from ERA5 over the GRACE record (2003-2022) and over the period 1951-1970, respectively. Observed monthly total precipitation over the GRACE record and over the period 1951-1970 is denoted by $P_{im}^{2003-2022}$ and $P_{im}^{1951-1970}$, respectively, and also obtained from the ERA5 dataset. Statistical uncertainty in $\Delta TWS_i^{historical\ warming}$ and $\Delta TWS_i^{historical\ wetting/drying}$ is characterised by re-calculating equation (4) and (5) for 1000 bootstrap estimates, blocked by basin, of $\widehat{\beta^{LR}}$ and $\widehat{\gamma^{LR}}$ and using these 1000 TWS change estimates to construct confidence intervals (CI).

Similarly, the total change in TWS in each grid cell i attributable to future climatic changes is estimated as follows:

$$(6)\ \Delta TWS_i^{future\ warming} = \widehat{\beta^{LR}}\left(\sum_{m=1}^{M} T_{im}^{2020-2050} - M\sum_{m=1}^{M'} \frac{T_{im}^{2003-2022}}{M'}\right),$$

$$(7)\ \Delta TWS_i^{future\ wetting/drying} = \widehat{\gamma^{LR}}\left(\sum_{m=1}^{M} P_{im}^{2020-2050} - M\sum_{m=1}^{M'} \frac{P_{im}^{2003-2022}}{M'}\right),$$

$\Delta TWS_i^{future\ warming}$ and $\Delta TWS_i^{future\ wetting/drying}$ denote the total projected changes in TWS until mid-century (from 2020 to 2050) due to climatic changes, relative to a counterfactual under a stationary climate defined as that observed over the 2003-2022 GRACE record. Climate projections are collected from five global climate models (GCM) from the Coupled Model Intercomparison Project Phase 6 (CMIP6) under the intermediate emissions scenario RCP4.5. For the purpose of this study the following GCMs are considered: GFDL-ESM4, IPS-CM6A-LR, MPI-ESM1-2-HR, MPI-ESM2-0, and UKESM1-0-LL. $T_{im}^{2020-2050}$ and $T_{im}^{2003-2022}$ are monthly average temperature in grid cell i obtained from the GCMs datasets over the period 2020 to 2050 and 2003 to 2022. $P_{im}^{2020-2050}$ and $P_{im}^{2003-2022}$ denote monthly total precipitation in each grid cell, from the five different GCMs employed, from 2020 to 2050 and 2003 to 2022, respectively. Statistical and climate model uncertainty in $\Delta TWS_i^{future\ warming}$ and $\Delta TWS_i^{future\ wetting/drying}$ is considered by re-calculating equation (6) and (7) for each combination of the 1000 bootstrap estimates, blocked by basin, of $\widehat{\beta^{LR}}$ and $\widehat{\gamma^{LR}}$ and the five different GCM datasets. The resulting 5000 estimates of $\Delta TWS_i^{future\ warming}$ and $\Delta TWS_i^{future\ wetting/drying}$ are then used to construct confidence intervals (CI).

To assess the impact of irrigation on observed and future TWS changes, the estimated irrigation-TWS relationship – $\hat{\delta}$ estimated from model (3) – is used. The effect of observed irrigation patterns on TWS trends over the last 20 years is calculated as follows:

$$(8)\ \Delta TWS_i^{historical\ irrigation} = (1)20 * \hat{\delta} I_i^{2000-2015},$$

with $\Delta TWS_i^{historical\ irrigation}$ representing the total change in TWS in each grid cell i over the 20 years of the GRACE record (2003-2022) attributable to observed irrigation and $I_i^{2000-2015}$ denotes the average annual fraction of area equipped for irrigation (AEI) in grid cell i calculated from observed irrigation data available for 2000, 2005, 2010, and 2015.[11] Similarly, the effect of future irrigation, considering irrigation expansion and contraction, is calculated through:

$$(9)\ \Delta TWS_i^{future\ irrigation\ expansion/contraction} = \hat{\delta}\sum_{y=1}^{Y} I_{iy}^{2020-2050},$$

where $\Delta TWS_i^{future\ irrigation\ expansion/contraction}$ is the total change in TWS in grid cell i until mid-century (from 2020 to 2050) due to irrigation. $I_{iy}^{2020-2050}$ denotes the simulated fraction of AEI in grid cell i in every year y over the period 2020-2050 obtained by extrapolating the historical linear trend in AEI. Statistical uncertainty in $\Delta TWS_i^{historical\ irrigation}$ and $\Delta TWS_i^{future\ irrigation\ expansion/contraction}$ is characterised by re-calculating equation (8) and (9) for 1000 bootstrap estimates, blocked by basin, of $\hat{\delta}$.

11 Piyush Mehta et al., "Half of Twenty-First Century Global Irrigation Expansion Has Been in Water-Stressed Regions," Nature Water 2, no. 3, March 2024, pp 254–61, doi:10.1038/s44221-024-00206-9.

App 3.3 Terrestrial moisture recycling (TMR)

Economic valuation

To assign a value to terrestrial moisture recycling (TMR) flows, it is essential to recognize that like other inputs to production, precipitation has declining marginal value to economic output. Therefore, the main and preferred set of metrics makes use of empirically estimated production functions that relate the quantities of precipitation in a given location and year to economic output. These production functions are typically in the quadratic form to capture the diminishing returns of increasing precipitation on economic productivity. The existing literature is used to employ such empirical estimates of the effect of precipitation on GDP growth rates (Damania, Desbureaux and Zaveri, 2020; Kotz, Levermann and Wenz, 2022) and agricultural production (Ortiz-Bobea et al., 2021). These estimated production functions are used to quantify the effect on these output variables from removing all precipitation in a destination location that is derived from terrestrial ET through TMR.

Figure 1 illustrates the method used to conduct this calculation. In each location, the estimated production function is used to assess by how much production would decrease if precipitation was reduced from the local climatic average by the contribution derived from TMR.

Formally, the following quadratic equation for each cell *i* globally is computed,

$$\Delta\ Growth_{\ i} = \beta_{precip}(P_{i,oceanic} - P_{i,total}) + \beta_{2\,precip}(P^2_{i,oceanic} - P^2_{i,total}) \quad (2)$$

Where $P_{i,oceanic}$ is the precipitation leftover after removing terrestrial-sourced precipitation and $P_{i,total}$ is the total precipitation (sum of both oceanic and terrestrial sourced precipitation) for cell i. β_{precip} and $\beta_{2\,precip}$ are the modeled quadratic parameters of economic growth and precipitation response function. Empirical estimates of these response parameters for GDPand agricultural output growth are obtained from the following studies:

	Estimate of β_{precip}	Estimate of β_{precip}^2	Study
Developing, GDP growth	3.684e-05	-2.653e-09	Kotz et al. (2022)
High-income, GDP growth	-2.59e-05	2.403e-09	
Developing, GDP growth	1.94e-05	-3.0e-09	Damania et al. (2020)
High-income, GDP growth	-2.64e-06	-8.70e-10	
Agriculture output growth	2.392e-04	-2.306e-07	Ortiz-Bobea et al. (2021)

FIGURE 1: Mapping changes in terrestrial precipitation to changes in GDP growth rates using established precipitation-GDP growth response functions.

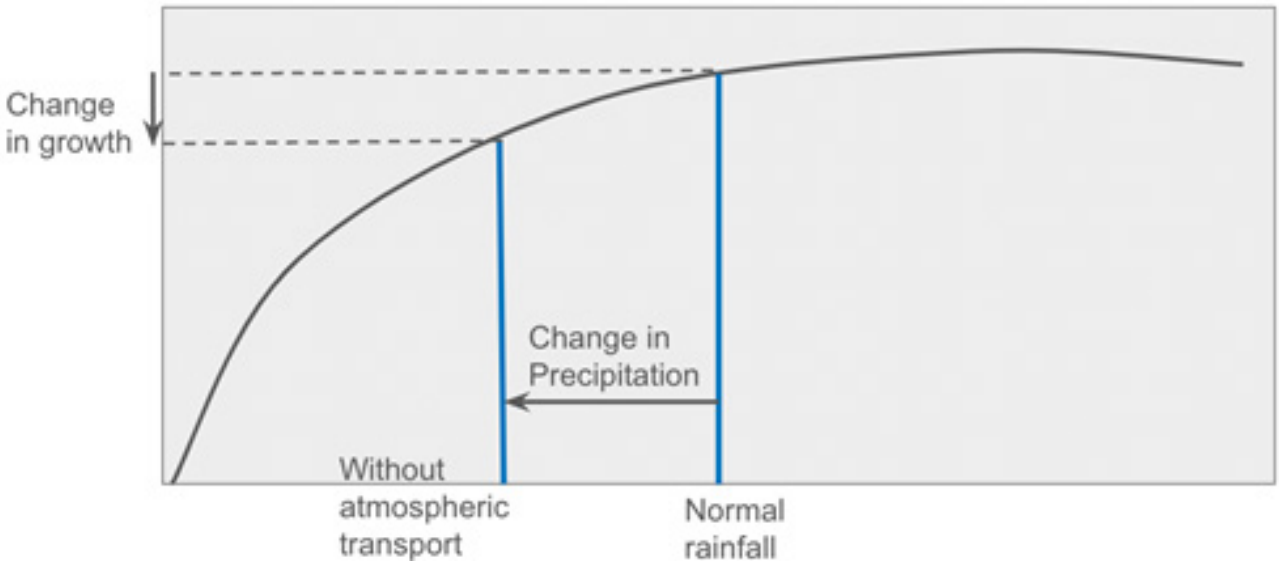

While the estimates are taken directly from Damania, Desbureaux and Zaveri (2020) and Ortiz-Bobea et al. (2021), the quadratic GDP growth-to-precipitation equation in Kotz, Levermann and Wenz (2022) is re-estimated after removing other measures of the precipitation distribution (such as annual days with extreme precipitation) to accommodate the aggregated nature of the UTrack AMF data.

The estimated changes in growth rates for each cell *i* are aggregated to the continent level. For all analyses, uncertainty from these empirical estimates is propagated by the delta method (maps) or bootstrapping (continental or country-level effects).

The bootstrapping procedure involved 1) re-estimating the parameters β_{precip} and β_{precip}^2 for each study, 2) calculating the impact for each cell *i*, 3) aggregating them to the country/continent level; and repeating the whole process 1000 times. The 95% confidence interval is obtained by identifying the 5th and 95th percentile of the country/continental impact distribution from 3).

Definition of deforestation hotspots by Harris et al., 2017

Throughout the report, the economic value of all AMR and AMR only from deforestation hotspots is considered. The term 'hot spot' is typically used to describe a region or value that is higher relative to its surroundings. In this report, the definition of a deforestation hotspot is adopted from Harris et al. (2017): a deforestation hot spot is an area that exhibits statistically significant clustering in the spatial pattern of forest loss. The Emerging Hot Spot Analysis was used to identify regions with significant spatial clustering of forest loss, taking into account the temporal dimension of forest loss in these clusters. First, spatial bins are clustered together by each bin's and its neighbours' forest cover loss measures. Neighbourhoods of statistically significant forest loss clusters are identified by the Queens Case Contiguity method. Second, the Emerging Hot Spot Analysis tool uses the Mann-Kendall statistic (Mann 1945, Kendall and Gibbons 1990) to test whether a statistically significant temporal trend exists through each bin's 14-year time series of Getis-Ord Gi* statistic. The Getis-Ord Gi* statistic is a measure of the intensity of clustering of high values (i.e. counts of forest loss) in a bin relative to its neighbour. Harris et al. then assigns each bin a deforestation category based on the cluster and its Getis-Ord Gi* statistic (e.g. intensifying to an increasing trend, persistent to a constant trend, and diminishing to a decreasing trend).

Appendix 3 - Additional figures and results

The table below shows a representative regression result of the climatic drivers of TWS changes:

TABLE 1: TWS differences on temperature and precipitation

Dependent Variable: **Model:**	**TWS (cm)** **(1)**
Variables	
Temperature (Celsius)	-0.0249***
Precipitation (cm)	(0.0086)
	0.0375***
	(0.0091)
Fixed-effects	
Grid cell	Yes
Basin-Year	Yes
Fit statics	
Observations	28,254
R^2	0.72723
Within R^2	0.08575

TWS differences are computed over 6 year time-periods Clustered (Basin) standard-errors in parentheses

Signif. Codes: ***: 0.01, **: 0.05, *: 0.1

The table below shows a representative regression result of the impact of irrigation on TWS changes:

Dependent Variable: Model:	*TWS* tr
Variables	
T anomaly (C) 1980-2000	
P anomaly (cm) 1980-2000	
Irrigated cropped area (fraction)	
Fixed-effects	
Basin	
Fit statistics	
Observations	
R^2	
Within R^2	

FIGURE A0: Agricultural productivity impact of removing terrestrial moisture flows originating from emerging deforestation hotspots.

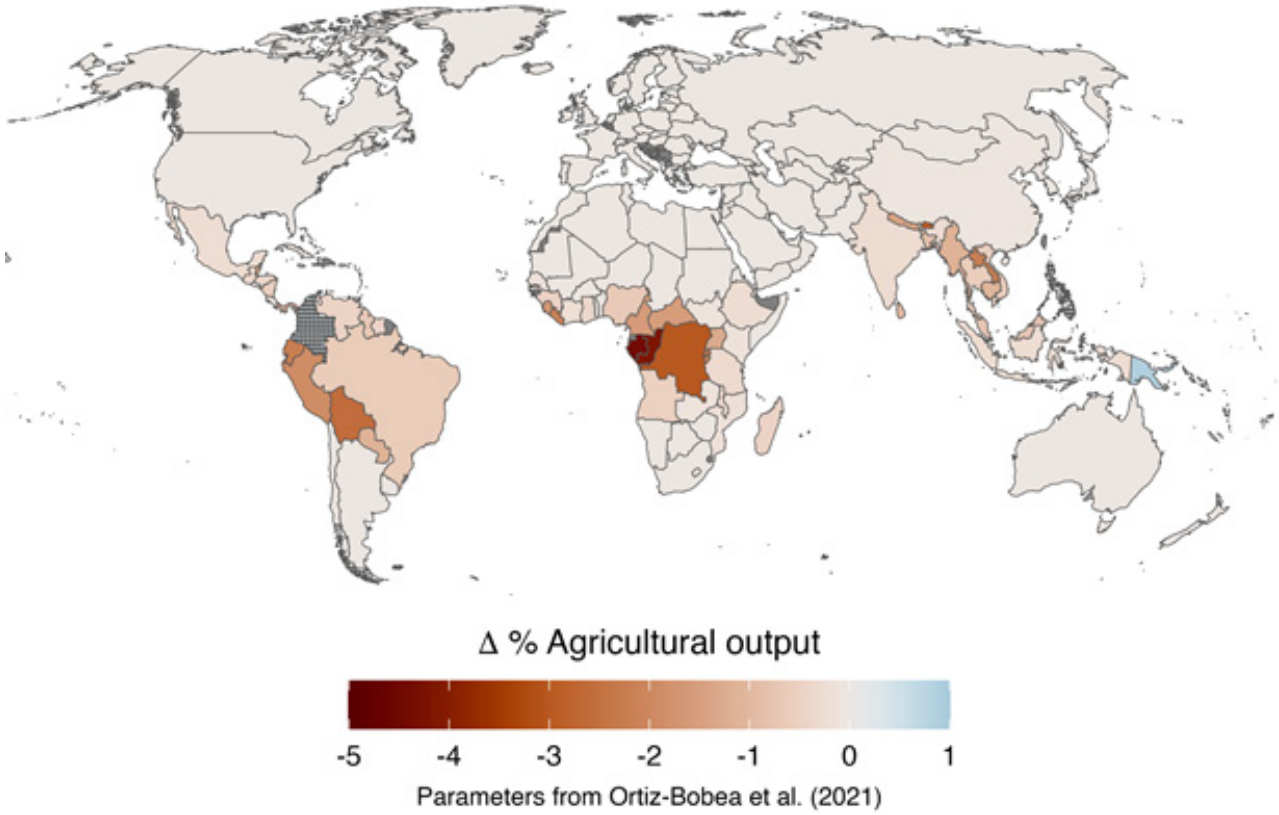

Note: Map plots the estimated change in agricultural output growth rates from removing terrestrial-sourced precipitation from emerging deforestation hotspots as defined by Harris et al., 2017. Outputs include crop and livestock commodities aggregated based on a common set of international prices derived by the Food and Agriculture Organization (FAO). Changes are calculated using estimates of the impact of historical precipitation on output from Ortiz-Bobea et al. (2021). Stippling indicates statistical uncertainty in the TFP growth rate change estimates at the country level using 95% confidence intervals obtained through bootstrapping.

FIGURE A1: Agricultural exposure to changes in total water storage.

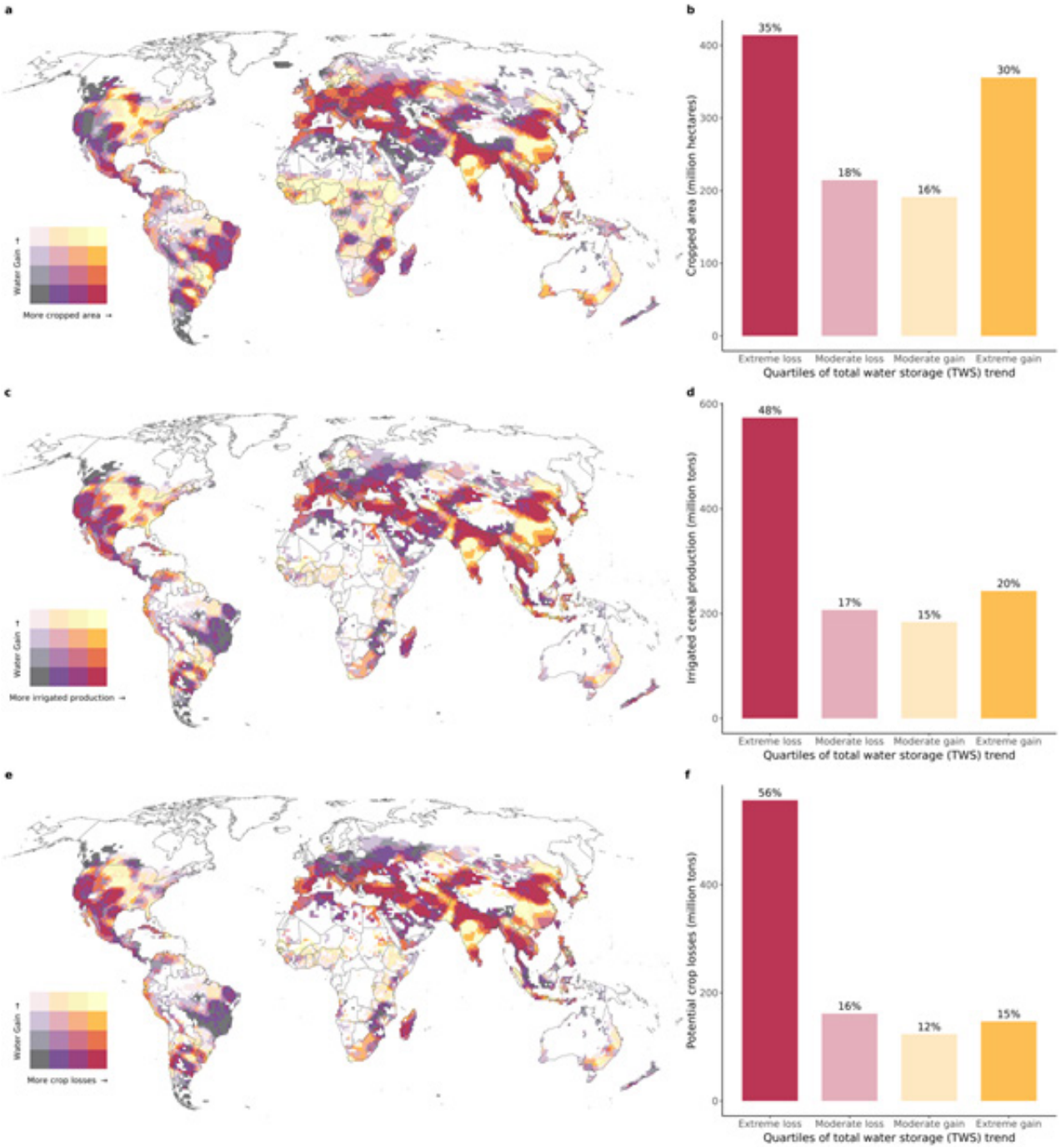

Note: Maps show trends in total water storage against: a, total cropped area from the Spatial Production Allocation Model (SPAM); c, irrigated cereal production from GAEZ, including wheat, rice, maize, sorghum, millet, barley and other cereals; e, potential cereal production losses if currently irrigated land would no longer be irrigated. Potential cereal production losses are assembled from GAEZ by calculating the difference between irrigated potential production and rainfed potential production in currently irrigated areas for wheat, rice, sorghum, millet, maize, and barley. All regions in white indicate non cropped land or no irrigated cereal production, respectively. Barplots show cropped area (b), irrigated cereal production (d) and potential cereal production losses (f) that fall into each quartile of the total water storage (TWS) trend distribution. Quartile 1 (denoted by extreme loss) contains TWS trends below -0.40 cm per year, quartile 2 (moderate loss) between -0.4 to -0.04 cm per year, quartile 3 (moderate gain) between -0.04 and 0.30 cm per year and quartile 4 (extreme gain) above 0.30 cm per year. Percentages indicate the share relative to total cropped area, total irrigated cereal production and total potential cereal production loss, respectively.

FIGURE A2: Changes in total water storage attributable to observed climate change.

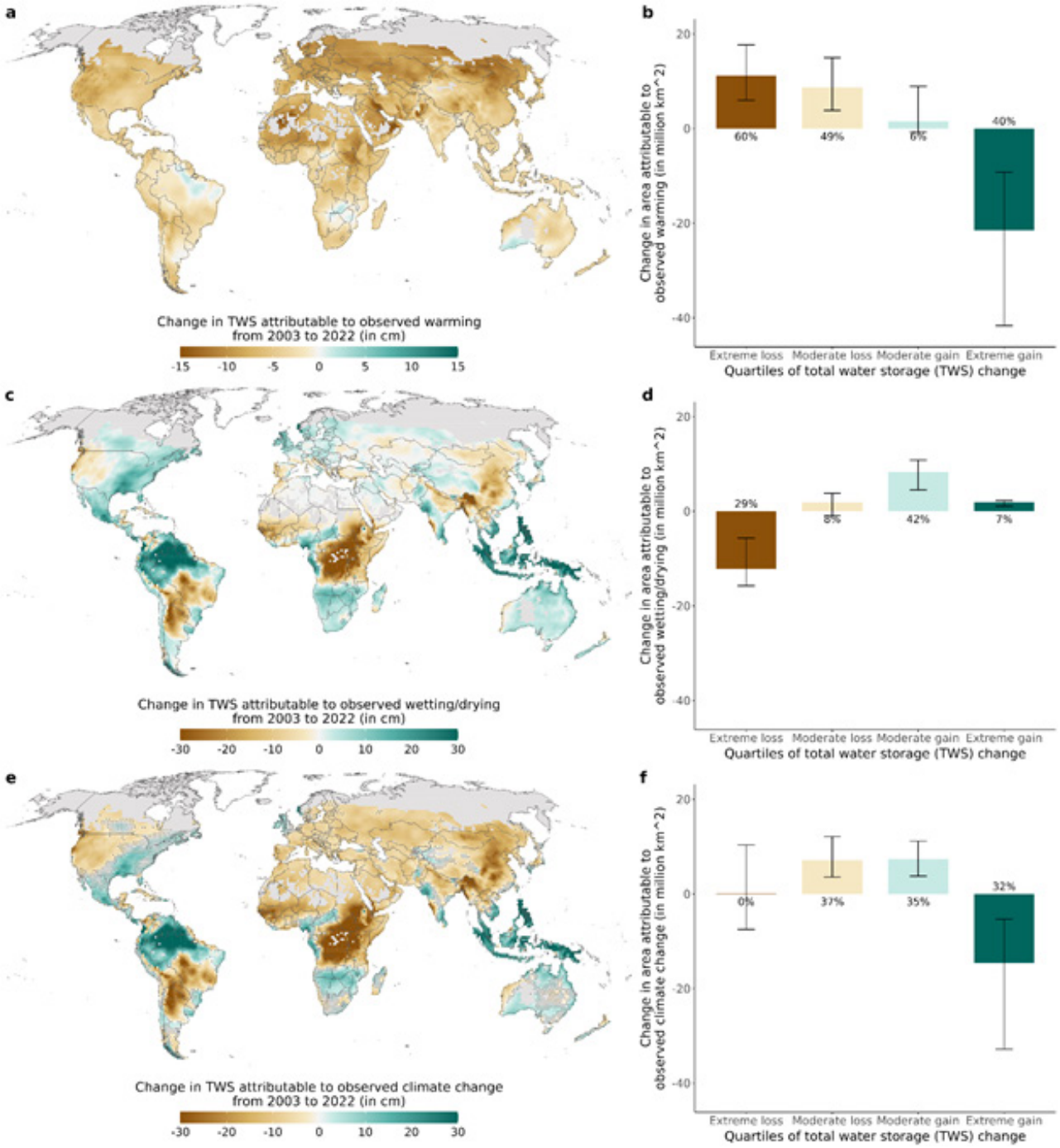

Note: Maps show the total change in total water storage (TWS) over the Gravity Recovery and Climate Experiment (GRACE) satellite record (2003-2022) in centimetres attributable to: a, observed warming; c, observed wetting/drying; e, observed warming and wetting/drying. Changes in TWS attributable to climatic changes are derived by combining observed changes in the climate obtained from the ERA5 reanalysis dataset with estimates of the TWS-temperature and TWS-precipitation relationship. Regions in grey have no arable land. Map stippling indicates regions where impacts of observed warming, wetting/drying, and climate change are not statistically distinguishable from zero, using a 95% confidence interval derived from block bootstrapping. Barplots show changes in arable land (in million km2) exposed to each quartile of the observed TWS change distribution due to warming and/or wetting/drying. Percentages indicate the percentage change in the area falling into each quartile due to observed climatic changes (relative to a counterfactual scenario with 1951-1970 climate). Quartile 1 (denoted by extreme loss) contains TWS trends below -0.40 cm per year, quartile 2 (moderate loss) between -0.4 to -0.04 cm per year, quartile 3 (moderate gain) between -0.04 and 0.30 cm per year and quartile 4 (extreme gain) above 0.30 cm per year. Colours indicate depletion (brown) and accumulation (green) of water resources due to observed climatic changes. Whiskers indicate 95% confidence intervals obtained through bootstrapping.

Future changes in total water storage

The estimated associations between TWS, irrigation, temperature and precipitation can also be used to project future changes to TWS. These projections are subject to many uncertainties; not only is the statistical model a simplified representation of a global average relationship between TWS, temperature, precipitation, and irrigation, but many factors could change these relationships in the future in ways that are very difficult to predict. For example, irrigation technologies may evolve, water infrastructure may change, or evapotranspiration may respond differently to climate forcing under a new equilibrium climatology. Thus, while these estimates provide data-driven, empirically-grounded estimates of what future TWS may look like under climate change, they should, like any future projection, be interpreted with caution. Under a moderate future emissions scenario (RCP4.5), it is estimated that human exposure to TWS is projected to accelerate dramatically by 2050. Climate changes over the coming three decades will decrease TWS in most areas (Figure 2.6), with global warming being the dominant driver of water loss in most regions (Appendix 3 Figure A3). The combined effects of temperature and precipitation under future climate change are likely to accelerate the declining global average trend in TWS over arable lands from a rate of -0.09 cm/year today to a rate of -0.28 cm/year (95% CI: -0.59 to -0.13) by 2050. Further, the share of arable land experiencing extreme water loss is estimated to increase by 50% (95% CI: 18-125%) under future climate change. Current levels of irrigation as well as further irrigation expansion could cause large water storage losses in isolated regions, particularly northern India and eastern China, both of which are key to food security today (Figure A5). Together, climate and irrigation drivers will increase exposure of vulnerable populations and agricultural production to extreme water loss in the future. For example, future irrigation will increase the share of irrigated cereal production exposed to extreme water stress globally by 50% (95% CI: 18-80%). Details on the socioeconomic impacts of hydrological imbalances caused by past and future climate change and irrigation are reported in Figure A6.

FIGURE A3: Estimates of projected water imbalances under future climate.

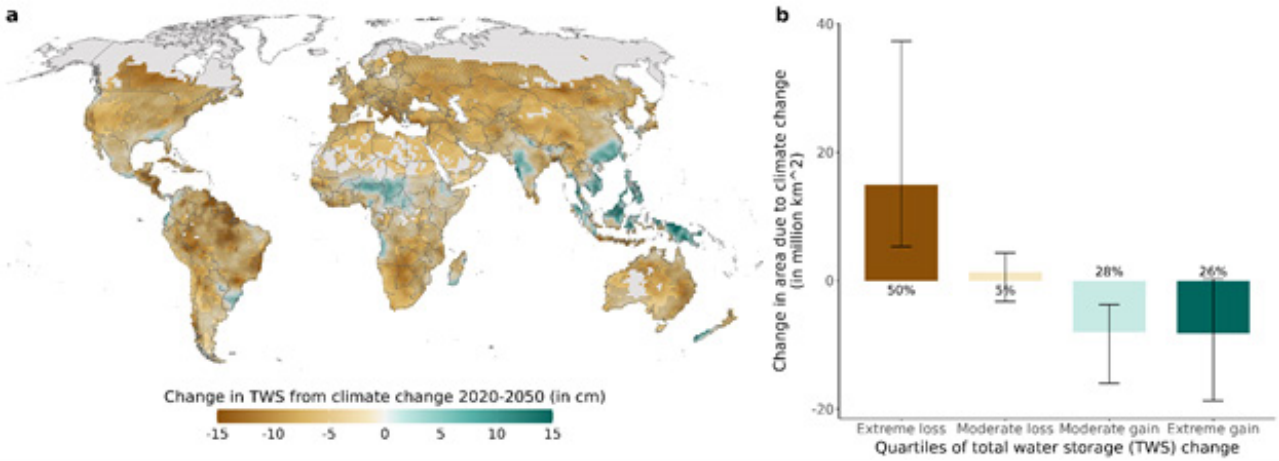

Note: a. The map shows estimates of projected total change in total water storage (TWS) over the period 2020 to 2050(in centimetres) due to future warming and wetting/drying. Changes in climatic conditions are projected using an ensemble of 5 global climate models from CMIP6 under RCP4.5. Projected changes in the climate, relative to the climatic conditions under a stationary climate defined as that observed over the 2003-2022 GRACE record, are combined with statistical estimates of the TWS-temperature and TWS-precipitation associations to derive changes in TWS attributable to future climate change (see Appendix 2 for details). Regions in grey have no arable land. Map stippling indicates regions where impacts of future climate change are not statistically distinguishable from zero, using a 95% confidence interval derived from block bootstrapping and considering climate model uncertainty. b. The barplot shows changes in the area of arable land (in million km2) that is exposed to each quartile of the observed TWS change distribution attributable to future temperature and precipitation trends. Percentages indicate the percentage change in the area falling into each quartile due to climatic changes (relative to a counterfactual scenario with a stationary climate defined as that from 2003-2022). Quartile 1 (denoted by extreme loss) contains TWS trends below -0.40 cm per year, quartile 2 (moderate loss) between -0.4 to -0.04 cm per year, quartile 3 (moderate gain) between -0.04 and 0.30 cm per year and quartile 4 (extreme gain) above 0.30 cm per year. Whiskers indicate 95% confidence intervals obtained through bootstrapping and by considering climate model uncertainty.

FIGURE A4: Water imbalances under future climate change.

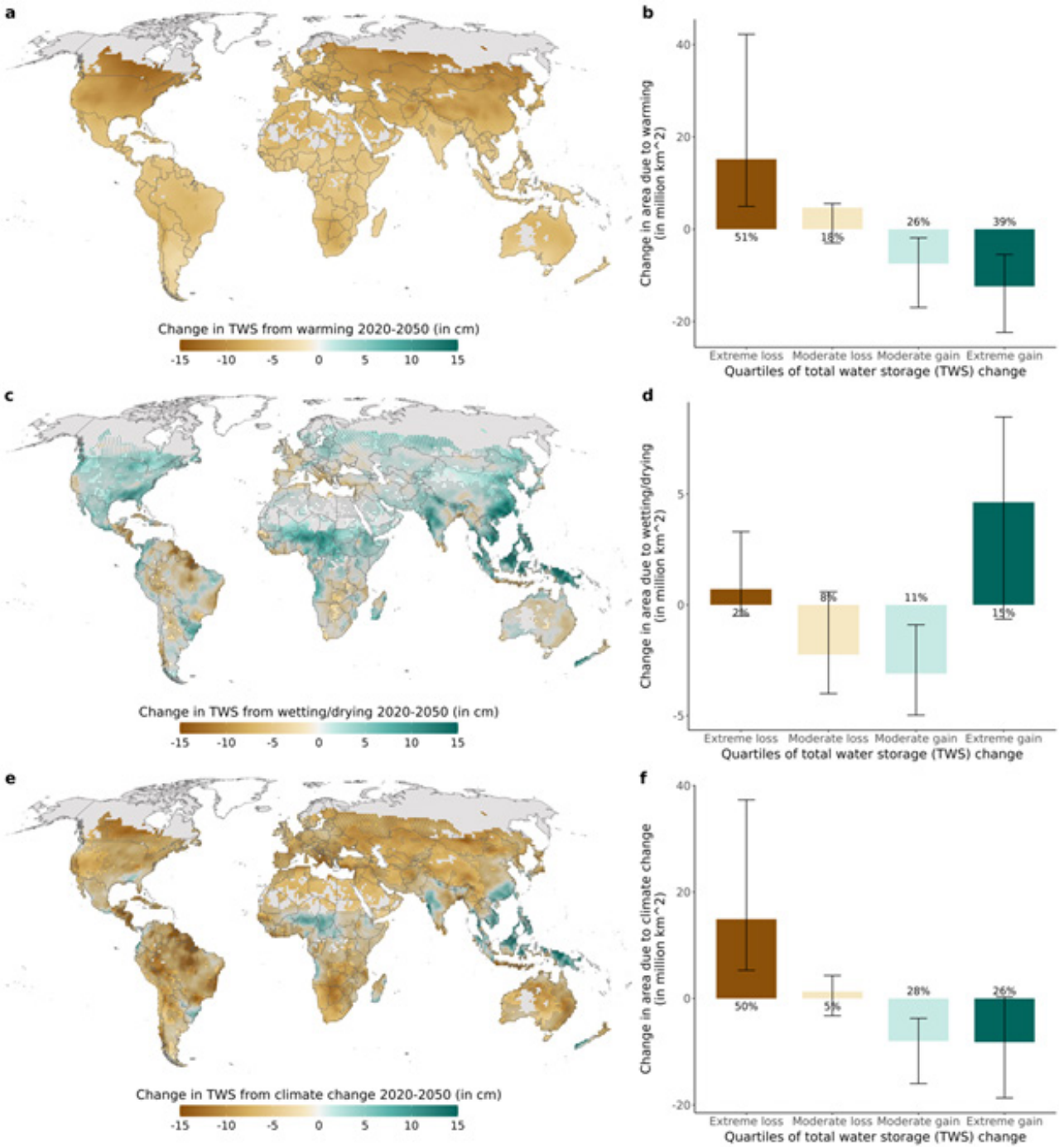

Note: Maps show the projected total change in total water storage (TWS) over the period 2020 to 2050 in centimetres due to: a, future warming; c, future wetting/drying; e, future warming and wetting/drying. Changes in climatic conditions are projected using an ensemble of 5 global climate models from CMIP6 under RCP4.5. Projected changes in the climate, relative to the climatic conditions from 2003 to 2022, are combined with estimates of the TWS-temperature and TWS-precipitation relationship to derive changes in TWS attributable to future climate change. Regions in grey have no arable land. Map stippling indicates regions where impacts of future warming, wetting/drying and climate change are not statistically distinguishable from zero, using a 95% confidence interval derived from block bootstrapping and considering climate model uncertainty. Barplots show changes in arable land (in million km2) exposed to each quartile of the observed TWS change distribution due to climate change. Percentages indicate the percentage change in the area falling into each quartile due to climatic changes (relative to a counterfactual scenario with a stationary climate defined as that from 2003-2022). Quartile 1 (denoted by extreme loss) contains TWS trends below -0.40 cm per year, quartile 2 (moderate loss) between -0.4 to -0.04 cm per year, quartile 3 (moderate gain) between -0.04 and 0.30 cm per year and quartile 4 (extreme gain) above 0.30 cm per year. Colours indicate depletion (brown) and accumulation (green) of water resources driven by climatic changes. Whiskers indicate 95% confidence intervals obtained through bootstrapping and by considering climate model uncertainty.

FIGURE A5: Water imbalances under future irrigation trends.

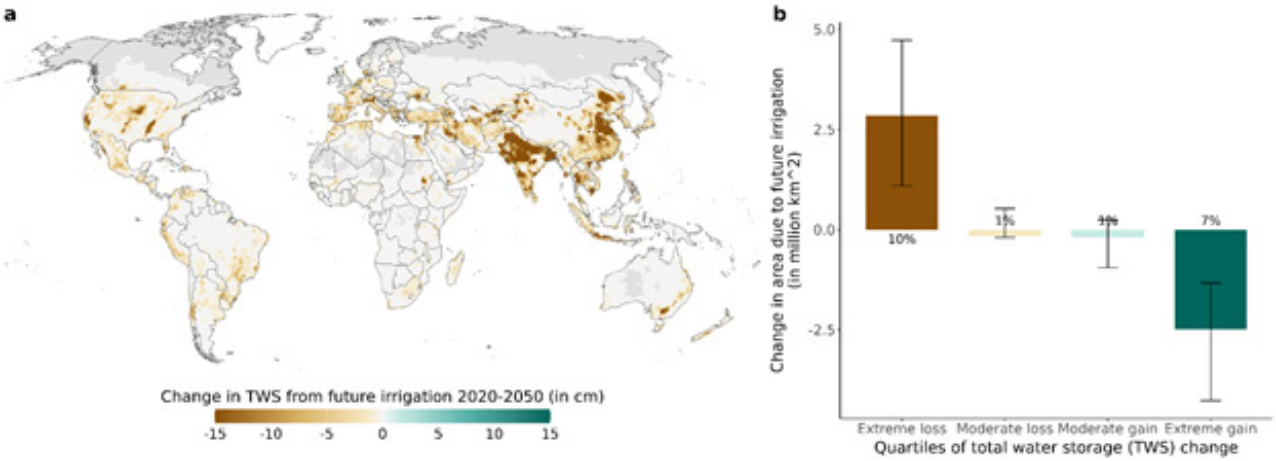

Note: a. The map shows the projected total change in total water storage (TWS) over the period 2020 to 2050 in centimetres due to the combined impact of current and future expansion in irrigation. Future irrigated areas are projected by extrapolating the trend in irrigated areas observed from 2000 to 2015 into the future. Projected irrigated area is combined with the estimated TWS-irrigation relationship to derive changes in TWS attributable to future irrigation. Regions in grey have no arable land. Map stippling indicates regions where impacts of future irrigation are not statistically distinguishable from zero, using a 95% confidence interval derived from block bootstrapping. b. The barplot shows changes in arable land (in million km2) exposed to each quartile of the observed TWS change distribution due to future irrigation. Percentages indicate the percentage change in the area falling into each quartile due to future irrigation (relative to a counterfactual scenario with no irrigation). Quartile 1 (denoted by extreme loss) contains TWS trends below -0.40 cm per year, quartile 2 (moderate loss) between -0.4 to -0.04 cm per year, quartile 3 (moderate gain) between -0.04 and 0.30 cm per year and quartile 4 (extreme gain) above 0.30 cm per year. Colours indicate depletion (brown) and accumulation (green) of water resources. Whiskers indicate 95% confidence intervals obtained through bootstrapping.

FIGURE A6: Historical and future risks to society.

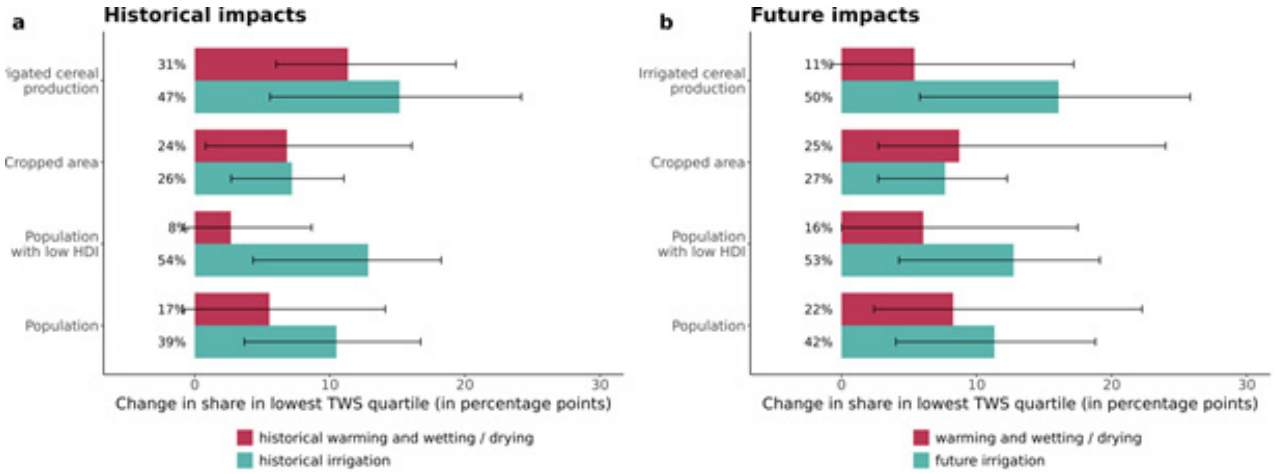

Note: The barplots shows the change in total people, vulnerable populations, cropped area, and irrigated agricultural production exposed to extreme water loss (lowest quartile of the observed TWS change distribution with TWS trends below -0.40 cm per year) attributable to historic and future climate change and irrigation. Historic changes due to observed climate change and irrigation are reported relative to a counterfactual under no historic warming and wetting or drying and no irrigation, respectively. Future changes are reported relative to the baseline exposure with observed TWS trends for assessment of the impacts of future climate change and relative to counterfactual exposure with no future irrigation. Impacts on four socio-economic variables are assessed: irrigated cereal production from GAEZ, total cropped area from the Spatial Production Allocation Model (SPAM), population in areas with human development index (HDI) below 0.7 from the Global High Resolution Estimates of the United Nations Human Development Index[12], total population from the Global Human Settlements Layer developed by the European Commission. Error bars indicate uncertainty (statistical and climate model uncertainty for the future climate change scenarios and statistical uncertainty for the historical and irrigation scenarios) in the exposure estimates using 95% confidence intervals obtained through bootstrapping.

12 Piyush Mehta et al., "Half of Twenty-First Century Global Irrigation Expansion Has Been in Water-Stressed Regions," Nature Water 2, no. 3, March 2024, pp. 254–61, doi:10.1038/s44221-024-00206-9.

FIGURE A7: Contribution of each land grid cell to global terrestrial precipitation.

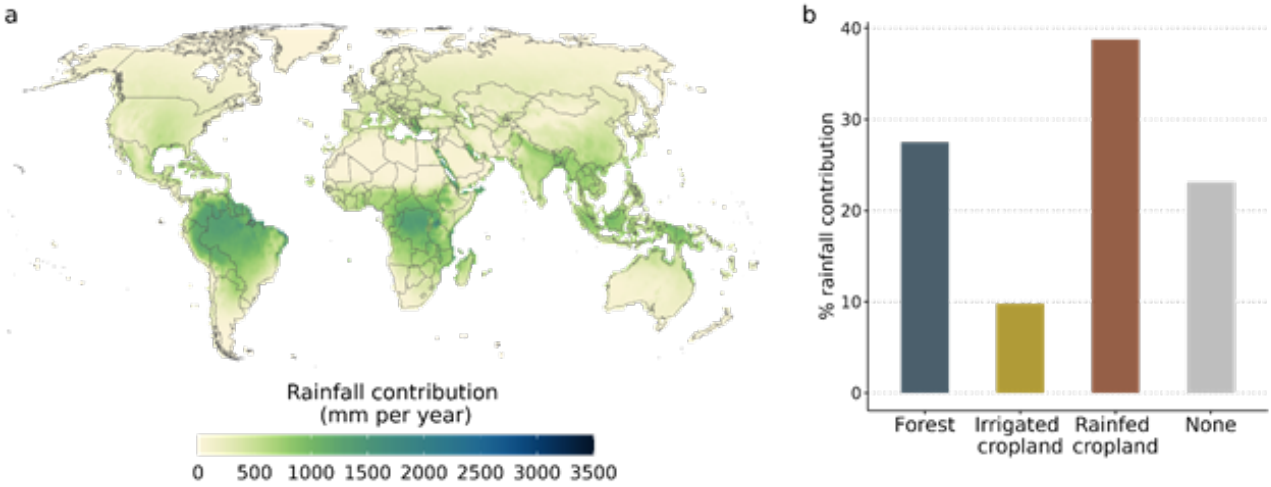

Note: a. The map shows the average annual amount of moisture generated by ET in each location over the period 2008-2017 that falls as precipitation on other terrestrial locations in mm per year. Darker green colours indicate more ET outflows to other terrestrial land. b. The barplot shows the share of total global terrestrial precipitation attributable to the three major categories of terrestrial sources of moisture (see Methods Appendix for a description of how moisture sources are categorised).

FIGURE A8: Economic impact of terrestrial moisture flow removal from all sources.

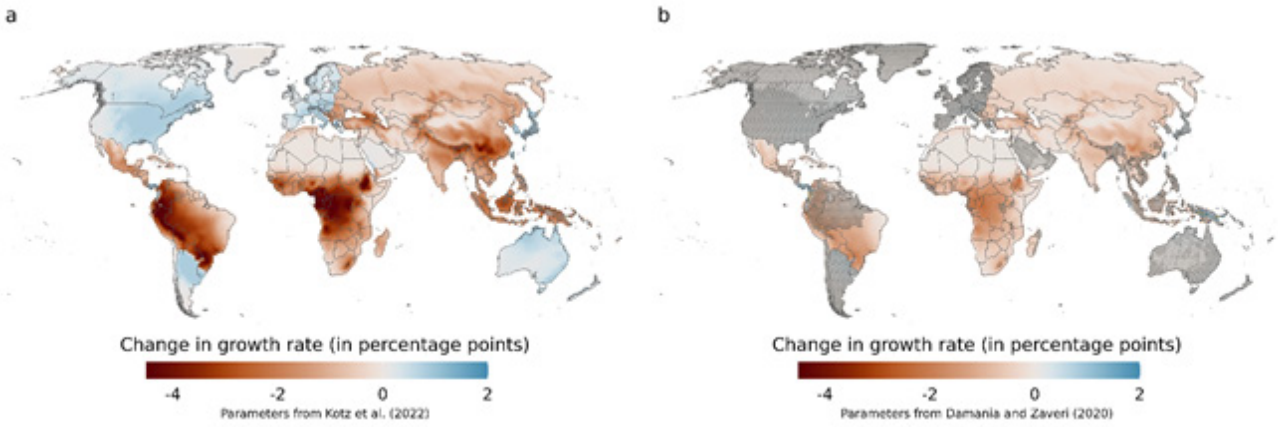

Note: Maps plot the estimated change in gross domestic product (GDP) growth rates from removing all terrestrial precipitation, effectively removing all moisture sources (e.g. forests, irrigated agriculture, and open water surfaces). Changes are calculated using estimates of the impact of precipitation shocks on economic growth from (a) Kotz, Levermann and Wenz (2022) and (b) Damania, Desbureaux and Zaveri (2020). Stippling indicates statistical uncertainty in the GDP growth rate change estimates using 95% confidence intervals obtained through the propagation of statistical uncertainty using the delta method.

FIGURE A9: Agricultural productivity impact of (a) all terrestrial moisture flow and (b) terrestrial moisture flows originating from emerging deforestation hotspots.

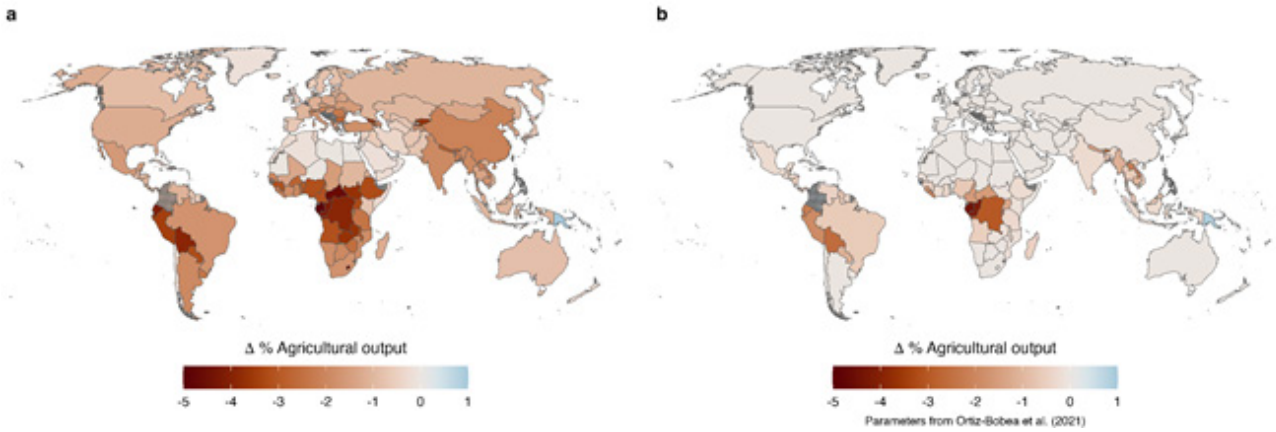

Note: Map plots the estimated change in agricultural output growth rates from (a) removing all terrestrial-sourced precipitation and (b) removing terrestrial-sourced precipitation only from emerging deforestation hotspots as defined by Harris et al., 2017. Outputs include crop and livestock commodities aggregated based on a common set of international prices derived by the Food and Agriculture Organization (FAO). Changes are calculated using estimates of the impact of historical precipitation on output from Ortiz-Bobea et al. (2021). Stippling indicates statistical uncertainty in the TFP growth rate change estimates at the country level using 95% confidence intervals obtained through bootstrapping.

App 3.4 Summary of the Empirical Evidence of the Effects of Precipitation on the Macroeconomy

It may seem obvious that rainfall has material impacts on the economy and hence variations in rainfall should emerge as a significant determinant of macroeconomic performance – at least in economies that are heavily dependent on rainfall. Yet much of the empirical climate change literature finds that precipitation has no effects on GDP while temperature increases have powerful negative effects in certain locations (e.g, Burke et al 2015). Likewise, much of the literature exploring whether rainfall has an impact on aggregate economic activity at a global scale, find no effect on GDP. Some even find no impact on agricultural GDP growth, though it is the sector that is most affected by rainfall (Barbier forthcoming).

Spatial aggregation of weather data at the country level explains why impacts of precipitation on GDP are found to be fragile. Rainfall and water availability exhibit considerable spatial variability that is considerably higher than that of temperature. Indeed, the wettest areas in Alaska (4,880mL year^{-1}) received 4,830mL more precipitation on average per year between 1990 and 2014 than the Mojave Desert (52mL year^{-1}). Such differences are also observed in the major urban centres of the USA with a difference of 1,800mL year^{-1} near Miami, Florida and 72mL year^{-1} in the Coachella Valley, California. And even higher spatial variability between the driest and wettest area is found in India (10,083mL year^{-1}), Colombia (7,138mL year^{-1}), Peru (6,518mL year^{-1}) or Papua New-Guinea (6,476mL year^{-1}). Temperature also varies within countries (e.g., a 40 °C difference between the coldest parts of Alaska and Miami, Florida) but globally, the within-country variation is twice as large for precipitation than it is for temperature. This implies that national level averages conceal much variation and hence generate results that do not represent what is happening in reality. For instance averaging rainfall in the Mojave desert with Alaska generates an unrepresentative statistic that is meaningless.

Note that at the smallest spatial resolution available (0.5 degree), there is an inverted U shape (concave) relationship between precipitation and GDP per capita growth. Rainfall increases total economic productivity, till it reaches a peak beyond which the marginal economic return declines with additional rainfall. The Figure on the left below plots the average cell-level precipitation (0.5 degrees) between 1990 and 2014 against the level of GDP per capita observed in 2014 (y-axis). Observe that precipitation and GDP per capita follows an inverted U-shape. Up to a level of 500mL to 700mL of precipitation, an additional drop of rainfall is correlated with a higher level of GDP per capita. The relationship then turns negative.

Now consider aggregating all of this data to the national level. The figure on the right shows the same plot but with data at the national level. The relation between rainfall and GDP has vanished and it is statistically insignificant. The results suggest the need for spatial disaggregation to capture local heterogeneity.

In general, stronger impacts of rainfall on GDP are found in developing countries, with greatest sensitivity and significance in cells with more than 75% cropland – confirming what is known, that agriculture is most directly impacted by rainfall variation. The literature also suggests what it is known that rainfall deviations from the average (shocks) are what matters most.

A common finding is that dry anomalies (1 or 2 standard deviations) are more harmful to GDP growth than are wet anomalies. Figure Y below summarizes such outcomes using GDP PC growth as the outcome variable. Similar results emerge using NPP (Zaveri et al 2020). Dry shocks are uniformly bad news and impact developing countries more. Small wet shocks are generally benign. However large wet shocks do take a heavy toll on developed and developing countries alike – shaving off around 0.3% of *growth.* Though impacts do not seem to highly statistically significant, due to generally good disaster risk management policies to address the damage brought by floods.

FIGURE A2: Precipitation and GDP at Different Spatial Scales.

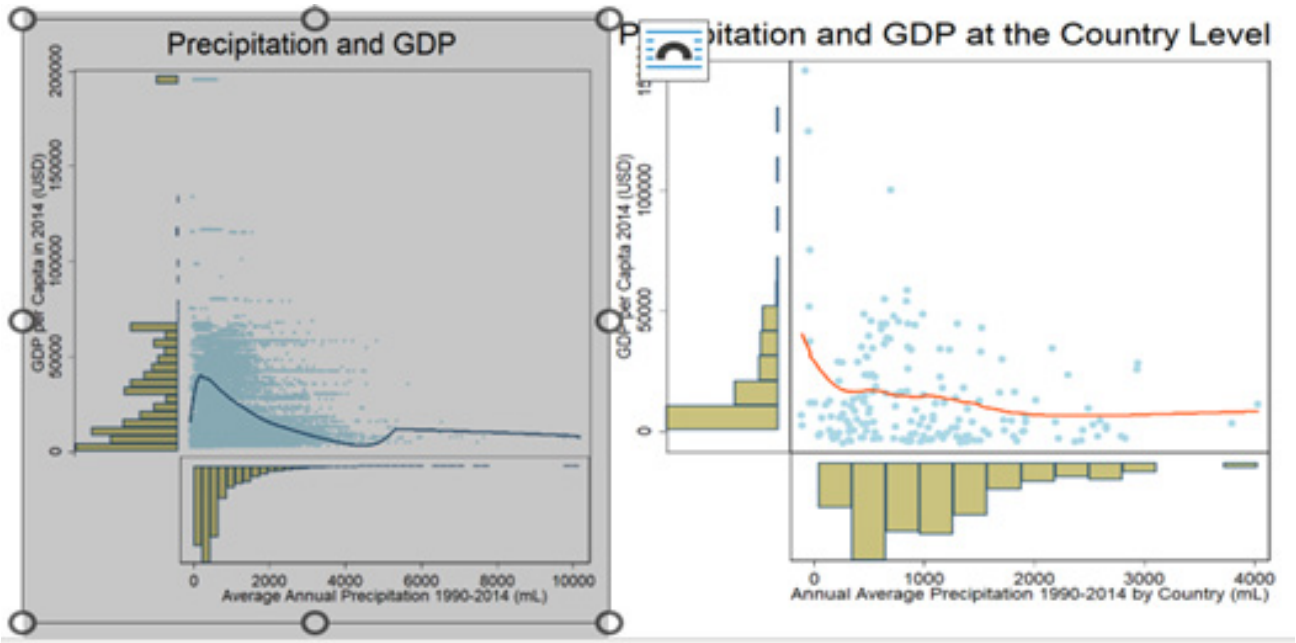

Source Damania, Desberaux and Zaveri 2020.

Notes The effects of rainfall on GDP vanish as aggregation increases. A case of the statistical issue known as MAUP (minimum area unit problem) .

FIGURE A3: Rainfall and GDP Growth.

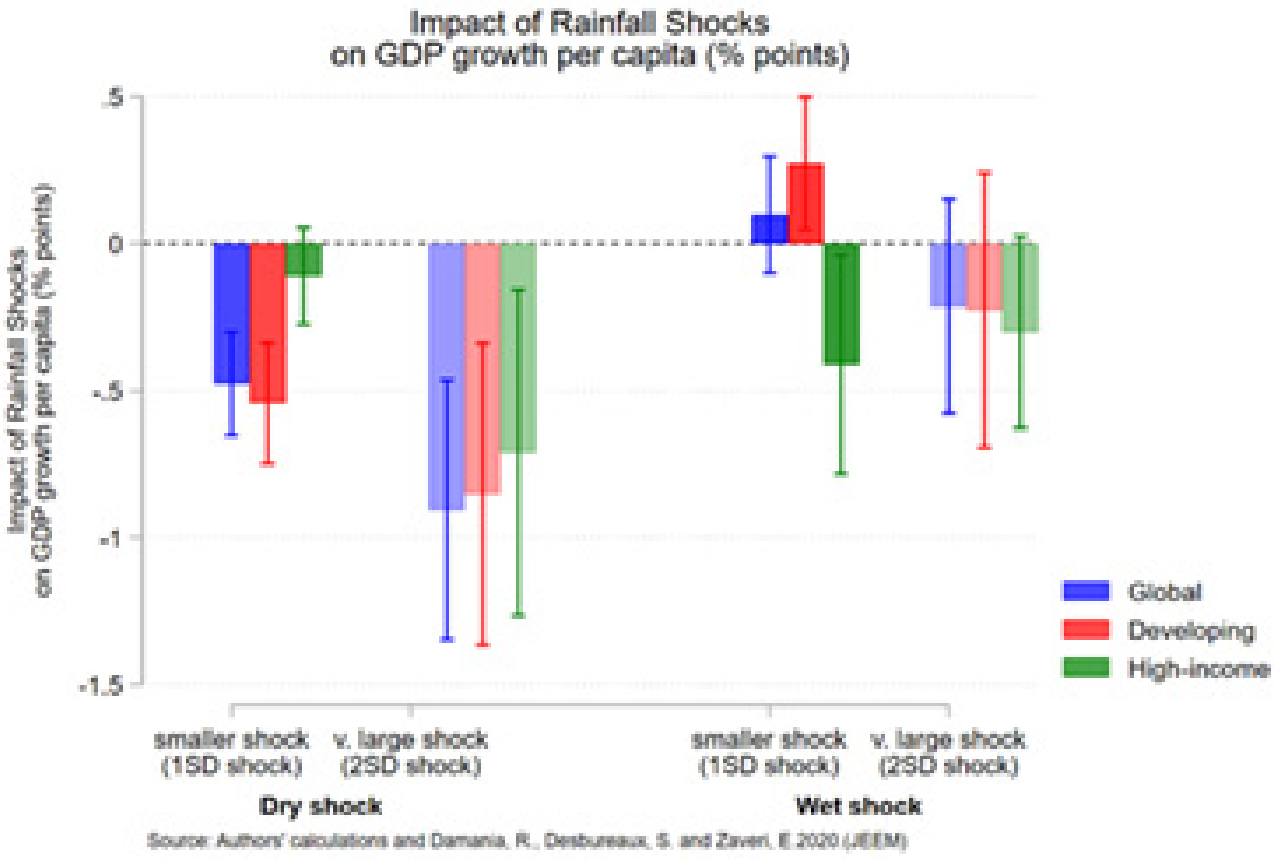

Notes Reduced form regression on GDP growth. Results show that dry anomalies of a given sd are more harmful than are wet anomalies and that developing countries are more impacted.

Summary of Estimates of the Effects of Climate Change on Income

The following figure from Tol 2024 synthesizes the range of GDP impact estimates under different scenarios and using different methods.

Estimates use a range of method: enumerative, models (CGE) and empirical. The enumerative approach omits price changes and interactions between sectors. Price changes and factor market interactions are at the core of computable general equilibrium models (CGE) and usually allow for endogenous adaptation. Reduced form econometric studies have the advantage that no assumptions are needed on the structure of the economy or how climate impacts segments of the economy or how they interact. But this requires valid causal identification which is easier for exogenous events like a rainfall shock than the more predictable changes (say in trends). A common finding in the literature across all approaches is that developing and warmer countries are worse impacted for well-known reasons – greater exposure to adverse events and trends and greater vulnerability to those impacts.

For comparison Figure A4 below shows the GDP effects when the explicit water related pathways are ignored. This would bring the model closer to a like-with-like assessment. The global impacts are around 5% which is extremely close to estimates obtained in other CGEs, with disproportionate effects on lower income countries.

FIGURE A3: Meta analysis of Economic Effects of Climate Change.

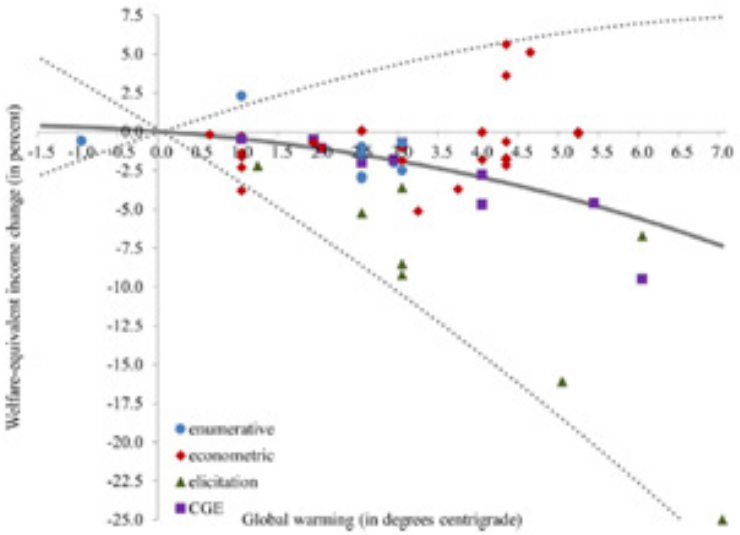

Fig. 1. The impact of climate change since pre-industrial times on global welfare according to comparative static studies.
Primary estimates are shown as dots. The central, solid line is the Bayesian model average, the dashed lines the central estimate plus or minus twice the estimated standard deviation.

FIGURE A4: GDP and Climate Change with Water Pathways Excluded.

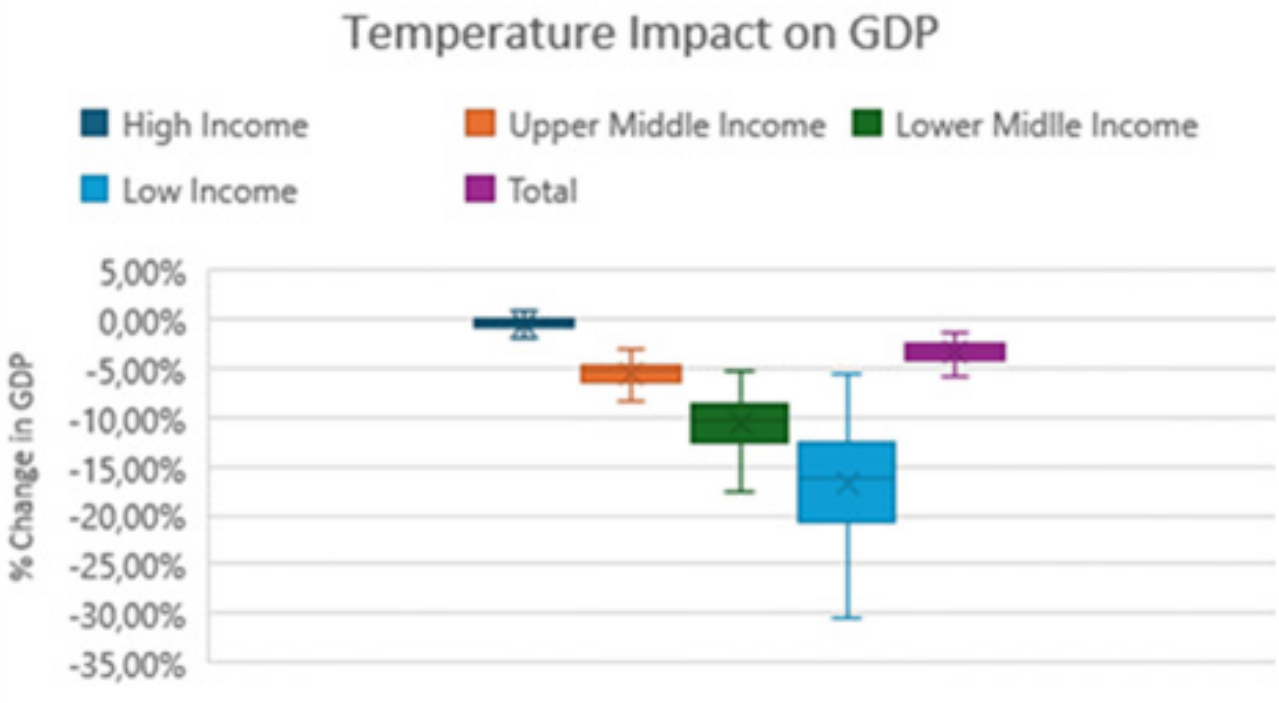

Source: Authors' calculations showing effects on GDP after 30 years with the explicit rainfall channels turned off. The results are close to those in other CGE studies.

References

Bredehoeft, J., and T. Durbin. "Ground Water Development—The Time to Full Capture Problem." Groundwater 47, no. 4, 2009, pp. 506–14. doi:10.1111/j.1745-6584.2008.00538.x.

Burke, Marshall, Solomon M. Hsiang, and Edward Miguel. "Global non-linear effect of temperature on economic production." *Nature* 527.7577 (2015): 235-239.

Cheng, Tat Fan and Mengqian Lu. "Global Lagrangian Tracking of Continental Precipitation Recycling, Footprints, and Cascades." J. Clim., vol. 36, no. 6, 24 Feb. 2023, pp. 1923-41, doi:10.1175/JCLI-D-22-0185.1.

D'Odorico, Paolo, Joel Carr, Carole Dalin, Jampel Dell'Angelo, Megan Konar, Francesco Laio, Luca Ridolfi, et al. "Global Virtual Water Trade and the Hydrological Cycle: Patterns, Drivers, and Socio-Environmental Impacts." Environmental Research Letters 14, no. 5, May 1, 2019, pp. 053001, doi:10.1088/1748-9326/ab05f4.

Fan, Y., H. Li, and G. Miguez-Macho. "Global Patterns of Groundwater Table Depth." Science 339, no. 6122, 22 Feb. 2013, pp. 940–43. doi:10.1126/science.1229881.

Harris, Nancy L., et al. "Using spatial statistics to identify emerging hot spots of forest loss." Environ. Res. Lett., vol. 12, no. 2, 7 Feb. 2017, p. 024012, doi:10.1088/1748-9326/aa5a2f.

Hoekstra, Arjen, and Mesfin Mekonnen. "The Water Footprint of Humanity." Proceedings of the National Academy of Sciences of the United States of America 109, February 28, 2012, pp. 3232–37, doi:10.1073/pnas.1109936109.

Keys, Patrick W., et al. "Invisible water security: Moisture recycling and water resilience." Water Secur., vol. 8, 1 Dec. 2019, p. 100046, doi:10.1016/j.wasec.2019.100046.

Kotz, Maximilian, et al. "The effect of rainfall changes on economic production." Nature, vol. 601, Jan. 2022, pp. 223-7, doi:10.1038/s41586-021-04283-8.

Mehta, Piyush, Stefan Siebert, Matti Kummu, Qinyu Deng, Tariq Ali, Landon Marston, Wei Xie, and Kyle Frankel Davis. "Half of Twenty-First Century Global Irrigation Expansion Has Been in Water-Stressed Regions." Nature Water 2, no. 3, March 2024, pp. 254–61, doi:10.1038/s44221-024-00206-9.

Rockström, Johan, Joyeeta Gupta, Dahe Qin, Steven J. Lade, Jesse F. Abrams, Lauren S. Andersen, David I. Armstrong McKay, et al. "Safe and Just Earth System Boundaries." Nature 619, no. 7968, July 2023, pp. 102–11, doi:10.1038/s41586-023-06083-8.

Rodell, M., J. S. Famiglietti, D. N. Wiese, J. T. Reager, H. K. Beaudoing, F. W. Landerer, and M.-H. Lo. "Emerging Trends in Global Freshwater Availability." Nature 557, no. 7707, May 2018, pp. 651–59, doi:10.1038/s41586-018-0123-1.

Sherman, Luke, Jonathan Proctor, Hannah Druckenmiller, Heriberto Tapia, and Solomon M. Hsiang. "Global High-Resolution Estimates of the United Nations Human Development Index Using Satellite Imagery and Machine-Learning." Working Paper. Working Paper Series. National Bureau of Economic Research, March 2023, doi:10.3386/w31044.

Tapley, Byron D., Srinivas Bettadpur, John C. Ries, Paul F. Thompson, and Michael M. Watkins. "GRACE Measurements of Mass Variability in the Earth System." Science (New York, N.Y.) 305, no. 5683 (July 23, 2004): 503–5. https://doi.org/10.1126/science.1099192.

Tol, Richard SJ. "A meta-analysis of the total economic impact of climate change." *Energy Policy* 185 (2024): 113922.

Tuinenburg, Obbe A. and Arie Staal. "Tracking the global flows of atmospheric moisture and associated uncertainties." Hydrol. Earth Syst. Sci., vol. 24, no. 5, 12 May. 2020, pp. 2419-35, doi:10.5194/hess-24-2419-2020.

van der Ent, Rudi J., et al. "Origin and fate of atmospheric moisture over continents." Water Resour. Res., vol. 46, no. 9, 1 Sept. 2010, doi:10.1029/2010WR009127.

Zaveri, Esha D., Richard Damania, and Nathan Engle. "Policy Research Working Paper 10453." *Policy* (2023).

App 3.5 CGE Modelling Details

The aim of this annex is to describe the construction of the economic model and the use of the inputs from the biophysical model both to estimate the extended SAM and the CGE parameters.

The CGE model (henceforth CLIMAWAT 101) has been built as the final step of an integrated system of sequential modules that proceeds from the construction of a database (economic, social and biophysical) to build SAM and CGE, to a gradual buildup of the various blocks of the model. The first stage of the sequence consists in compiling the database from GTAP 11, national accounts, economic and social statistics, and data from FAO and the Water Footprint Network. The second stage is the construction of a global social accounting matrix, integrating all information at country level with intercountry data on trade. This includes the accounting for blue and green water and their multiple uses as natural resources, primary factors of production and intermediate inputs. In a third stage, water is integrated into the system by using a system of bridge matrices (BMA) that are capable to transform biophysical estimates in different units directly and interactively into SAM and CGE parameters. The BMAs include the data sets by year and geographic location of each variable (e.g. blue and green water withdrawals and consumption, agricultural yields and prices, health damage etc.) and the functions mapping them into estimates of SAM coefficients and/or model parameters.

CLIMAWATT, the CGE (Computable General Equilibrium) model developed for this exercise offers a detailed representation of the world economy, encompassing 160 countries and 14 production sectors along with their corresponding commodities. This model integrates data from numerous international statistical sources, such as GTAP 11, FAO, and the Water Footprint Network. It also incorporates inputs from biophysical models, economic databases, econometric estimates, and climate change projections.

The model simulates a global system of economic agents, including consumers, producers, and governments, who operate within interconnected markets. In these markets, all endogenous variables, such as prices and quantities, are jointly determined. Key parameters within the model include production and utility functions, input-output coefficients, income shares of consumption across different commodities, and shares and elasticities of substitution for land, labor, capital, and water across various sectors and locations. Green water impacts total factor productivity in agriculture, while blue water is modeled as a “primary resource” and an input in production, acknowledging its explicit or implicit use in all economic activities. Additionally, the model accounts for unemployment and can distinguish between high and low income and skill categories. This capability allows for a nuanced analysis of labor market dynamics and income distribution effects.

The model solutions offer a robust framework for investigating how markets adjust to exogenous shocks, with comparative static-steady state equivalents that can be compared to the Balanced Growth Equivalents (BGEs) used in the Stern Review. To provide a more concrete reference for the scale and timing of changes, the “snapshots “ obtained solving the model are projected over a 30-year timeline using OECD investment and population forecasts as exogenous variables. This approach enables an examination of long-term economic impacts and the interplay between various factors in the context of global economic and environmental changes.

The core of the CGE model follows Robinson (1999) and Logfren (2001), Thierfelder et al. (2017), reformulated (Damania and Scandizzo, 2016, Damania et al, 2019, Cervigni and Scandizzo, 2017, Perali and Scandizzo, 2018) to consider the externalities from climate change and water consumption. Two-level nested CES functions are utilized to define the substitution possibilities between labor, capital, land, water, and intermediate inputs. The corresponding substitution elasticities are initially derived from the literature and subsequently refined through iterative calibration. Each sector produces a composite commodity that can be either exported or produced for the domestic market. All producers for each region are assumed to maximize profits according to a production function, which uses primary and intermediate inputs, under the assumption (bounded rationality) that the level of use of some of these inputs are fixed by technology or by former uses. Each producer runs a production activity with the end result of supplying one or more commodities with labor, capital land and Natural Resources as primary inputs, which are determined by Constant Elasticity of Substitution (CES) production functions. The demand for intermediate inputs assumes fixed

input-output coefficients and the demand for primary factors is given by first order condition for profit maximization using value-added prices. Blue Water is both a commodity used by activities as an intermediate input, and produced and distributed by specific activities, such as water companies and utilities, and a natural resource used as a primary input. Green water is a natural resource whose exogenous supply affects total factor productivity of agricultural activities. Production is either for regional domestic market or for trade/exports to international market, according to a Constant Elasticity of Transformation (CET) function, where (i) producers maximize revenue from sales subject to the CET function and (ii) export supply represents the first order condition and is a function of the elasticity of transformation, the share parameter in the function and the relative export price to domestic price. The allocation of imports and domestic production is determined according to CET functions, where import demand represents the first order condition for minimizing the cost of buying a given amount of composite good. These functional forms (CET and CES) assume imperfect substitution and transformation between imports, exports and domestic goods and imply assumptions about separability and absence of income effects, where the ratios of exports and imports to domestic goods depend only on relative prices.

Although the model has a neoclassical structure, in terms of agents' optimization and market equilibrium, these conditions are used as a micro-foundation for the application of Keynesian closure rules to account for unemployment and investment multipliers. The technology for producers and consumers is described by CES functions and consumption demands are derived assuming that optimization is successful but can also be hampered by lack of information or other constraints. Commodities are either sold in the domestic markets or exported to international markets. CET functions describe the relationship between the internal and external markets, with the determination of price ratios and elasticity of transformations to determine the levels of output exported or sold domestically. Government inflows are represented by taxes and transfers from other institutions and at the same time use the income to purchase commodities, make transfer to other institutions and savings. The commodities demanded by governments are determined in fixed proportion and transfers from and to other institutions are also fixed in foreign currency. Institutions also include enterprises, that receive inflows from factor of production and transfers from other institutions. As outflows, the income of enterprises is used to pay taxes, savings, and transfers and to consume commodities.

CLIMAWAT incorporates modules to simulate the impact of the externalities such as morbidity and mortality due to inadequate water supply, hygiene, and sanitation (WASH), based on data from the WHO database. Data on Bluewater and Green water consumption have been obtained from the Water Footprint Network (Mekonnen and Hoekstra 2011), for agriculture and livestock, industrial and domestic consumption. Other water data have been taken from FAO Aquastat database, in particular for what concerns water withdrawal, both for surface-water and groundwater. Data on water requirements and water tariffs are taken from the FAO data base and the literature.

Countries are first divided into 10 subregions, according to geographic location, and then further divided according to World Bank income group classification (Low-income, Lower-Middle Income, Upper-middle Income, High Income). As a result, the model encompasses up to 40 distinct regions along with an aggregate category for the "Rest of the World" (ROW) to ensure comprehensive global coverage. To simulate the impact of climate change to the economy, data from The Potsdam Institute for Climate Impact Research (PIK) are combined with different regression estimates from the literature (Ortiz-Bobea et al. (2021) and Damania et al. (2020)).

Thanks to its dynamic calibration, the model can accurately adjust to any base year from 2007 to 2017, meeting researchers' needs for flexibility and preventing excessive results' dependence on a limited calibration basis. This adaptability, facilitated by the panel nature of the GTAP dataset, appears also to improve the model performance in predicting the recent evolution of the global economy, as evidenced by the Figures below.

FIGURE 1: Model Simulations of Baseline GDP by Region.

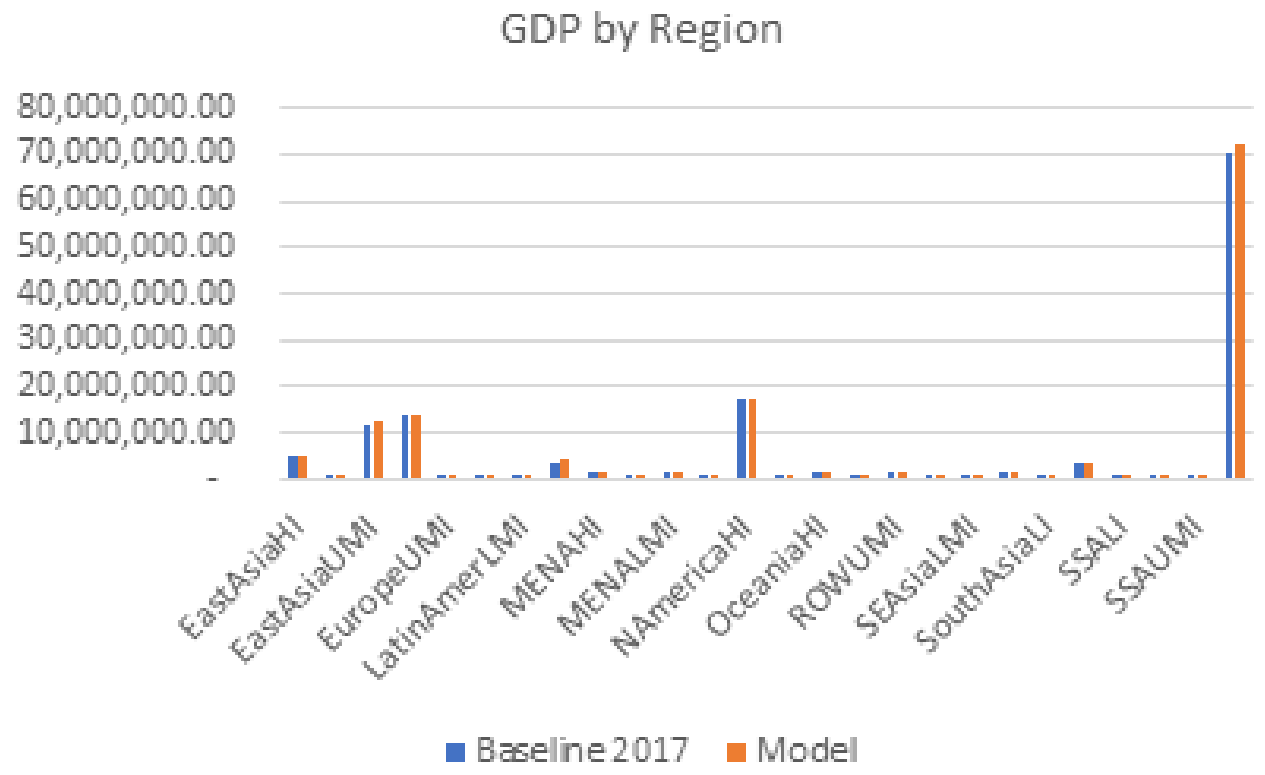

FIGURE 2: Model simulation of WDI2018 GDP by region.

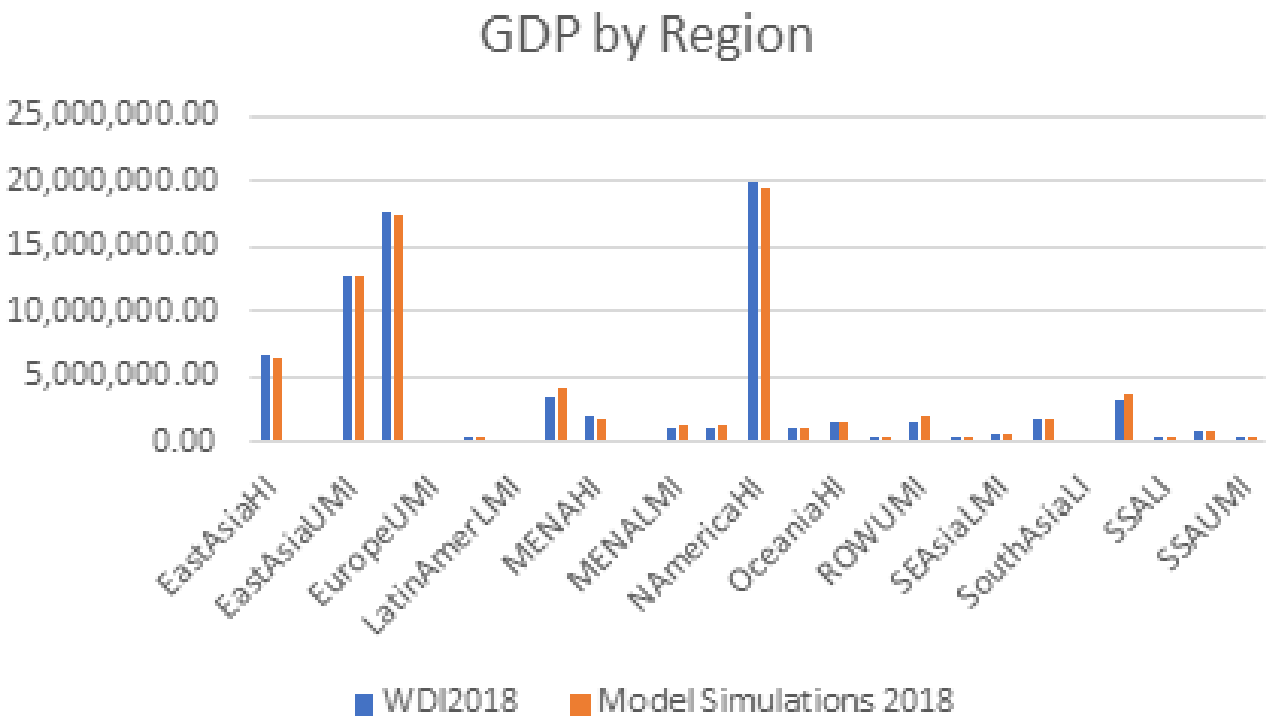

FIGURE 3: Comparative Model Performance on two Data sets.

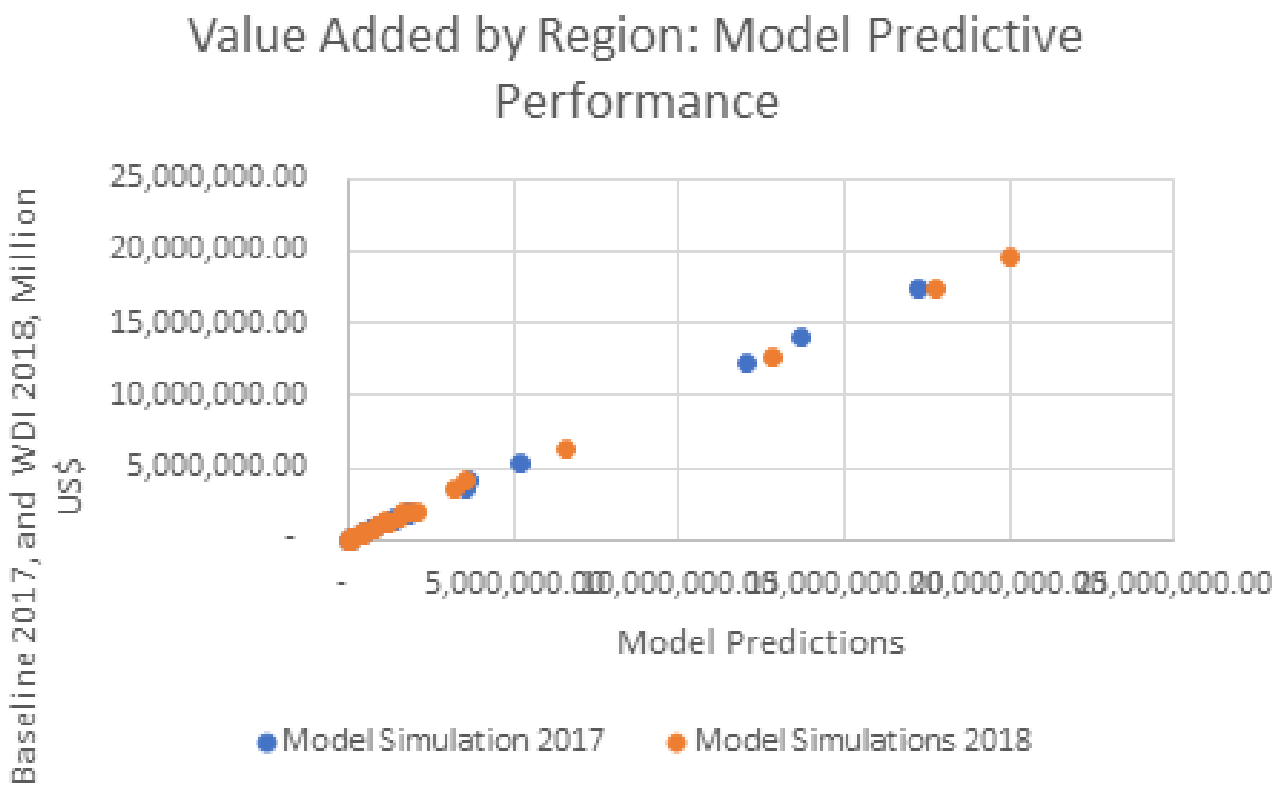

The above figures illustrate the model's predictive performance for value added by region, comparing model simulations with baseline data for 2017 and World Bank WDI data for 2018. In Figure 3, the blue dots represent the 2017 model simulations, while the orange dots correspond to the 2018 model simulations. The alignment of the dots along the diagonal line indicates a strong predictive capability of the model, demonstrating its accuracy in capturing the recent evolution of the global economy. This performance is achieved through dynamic calibration, allowing the model to adjust effectively to various base years within the 2007-2017 period. The close proximity of the dots to the diagonal suggests the model's reliability in forecasting value added across different regions.

References

Aldaya, M. M., Chapagain, A. K., Hoekstra, A. Y., & Mekonnen, M. M. (2012). The water footprint assessment manual: Setting the global standard. Routledge.

Cervigni, R. and Scandizzo, P.L. eds, (2017), The Ocean Economy in Mauritius, Making it Happen, Making it Last, The World Bank

Damania, R., Desbureaux, S., & Zaveri, E. (2020). Does rainfall matter for economic growth? Evidence from global sub-national data (1990–2014). Journal of Environmental Economics and Management, 102, 102335.

Damania R., Desbureaux S., Scandizzo, P., Mikou M., Gohil D., Said M. (2019), When Good Conservation Becomes Good Economics: Kenya's Vanishing Herds, World Bank

Damania R. and Scandizzo, P.L. (2016), "The Serengeti ecosystem—Burden or bounty?" Journal of Policy Modeling.

Lofgren, H, Harris, G & Robinson, S, 2001: A Standard computable general equilibrium (CGE) model in GAMS, International Food Policy Research Institute, Trade and Macroeconomic Division, Discussion Paper no 75.

Ortiz-Bobea, A., Ault, T. R., Carrillo, C. M., Chambers, R. G., & Lobell, D. B. (2021). Anthropogenic climate change has slowed global agricultural productivity growth. Nature Climate Change, 11(4), 306-312.

Perali, F. and Scandizzo, P.L.,eds(2018), The New Generation of Computable General Equilibrium Models, Springer, 2018

Appendix 5.1

Examples of innovations relevant to the five critical water missions

Box 1: Water productivity of rice can be increased

Rice is the world's staple crop, taking up 11% of the world's cultivated land. In Asia, irrigated rice accounts for 80% of the freshwater utilised for irrigation [1]. Traditionally, continuous flooding is utiltised for irrigation, resulting in large amount of unproductive water outflows through evaporation, seepage and percolation. Techniques are available to reduce water consumption and increase productivity.

***Alternate Wetting and Drying** (AWD) allows water levels in irrigated rice fields to naturally decrease before irrigation. This controlled, intermittent irrigation technique has allowed for up to 20% - 30% water savings in rice farming in Bangladesh, compared to traditional flooded cultivations [2]. By reducing costs relating to water pumping and fuel consumption, it has also increased the income of farmers – by 38% in Bangladesh, 32% in the Philippines and 17% in southern Vietnam [3].*

***Direct seeding** involves having the rice seed sown and sprouted directly into the field, as compared to sprouting it in a nursery and transplanting the sprouted seed into standing water. This reduces water consumption by up to 12%, and produced higher yields of up to 18% compared to traditional transplanted rice in field studies in Punjab, Pakistan [4]. It can reduce labour requirements by up to 60%, resulting in a lower cost of production and higher economic return [5].*

***Rice-shrimp rotation** is an intercropping farming practice which provides an integrated model to improve farmer's incomes and resilience. Shrimp are grown in the dry season and periods of saltwater intrusion, while rice is farmed in the rainy season when residual salinity is flushed. Both systems provide mutual ecosystem benefits – nutrients that accumulate in sediments during the shrimp culture period are beneficial for rice growing; in turn, rice plants help clear pond mud, which supports shrimp health. [6] While this has been an ancient practice in the Mekong Delta, the sustainable farming model is gaining traction and promoted as a form of adaptation to climate change and sea-level rise. The Minh Phu Seafood Corporation, Vietnam's largest shrimp producer, has been scaling up the sustainable rice-shrimp model from its initial pilot partnership with World Wildlife Fund and the Dutch Fund for Climate and Development. The benefits to yield and income are multi-fold: 4-fold increase in shrimp production; 3.5 times increase in income with growing international demand for sustainable shrimp in Europe and the United States. [7] It is also expected to support the health of the delta by increasing its depth by 4 to 6cm, reversing land subsidence.*

Box 2: Harnessing data for efficient agriculture

*In Phú Cần province, Vietnam, a local farming co-operative and Tra Vinh University piloted the use of **solar-powered sensors**[13] to allow farmers to monitor water levels in their rice fields via smartphones. The sensors allow for the optimisation of Alternate Wetting and Drying; pumps were utilised only three to four times per season, a sharp reduction from 10 times per season using flood irrigation [8]. For the same amount of rice, use of sensors has reduced the amount of water (up to 20%) and electricity used. It also required less labour, resulting in an increase in productivity.*

*Precision irrigation can be combined with combinations of soil and weather health data, such as soil moisture sensors, satellite data. **Soil-moisture sensors** aid in irrigation management by measuring the moisture of soil at different locations and depths, providing data to optimize irrigation schedules and*

13 These sensors take a reading of the underground water level every five minutes.

amounts. ***Satellites imagery,*** *in combination with meteorological data, can help estimate parameters such as leaf area index, plant density which can help to monitor water demand on a large scale basis.*

Agrinex, a ***smart drip irrigation technology*** *utilises a mesh-based Wireless Sensor and Actuator Network (WSAN), which aims to enhance resource efficiency and crop yields through a dynamic network of in-situ sensor nodes that monitor soil moisture, temperature, and humidity, paired with actuators for controlled drip irrigation [9]. Agrinex achieved 81% in water savings without compromising crop yield potential [9].*

FarmiSpace, a platform established by DataYoo, a leading agritech company, provides ***satellite data*** *to monitor their feels daily, detecting subtle changes in crop health, water stress and growth patterns. Priced at USD $42/year, the platform democratises access to advanced agricultural technology to smallholder famers [10]. Digital field management enables farmers to precisely monitor crop metrics, make scientific and systematic field decisions, and apply field data across various applications, such as integrating farm machinery operations. Farmers can set warning thresholds on FarmiSpace, which, combined with satellite data, can generate monitoring reports identifying pest infestations or abnormal crop conditions [11]. The alerts allow farmers to take timely action before situations worsen, such as decreasing plant moisture levels or a high proportion of diseased plants.*

The LARI Lab phone application, a collaboration between the Lebanese Agricultural Research Institute and the International Water Management Institute, provides Lebanese farmers with ***customised information to their plots, weather conditions and crop types*** *[12]. For instance, the app integrates geo-specific weather data and crop evapotranspiration values, and translates that into customised irrigation schedules for the farmer, based on crop type, irrigation system and soil type. The app also provides farmers with information about how much they need to irrigate in the next 7 days, as well as details on crop evolution and health using FAO's open-access portal for monitoring water productivity.*

Box 3: Alternative irrigation and rainwater harvesting techniques have been shown to work in several contexts.

Micro-irrigation[14] *reduces water consumption compared to conventional flood irrigation by avoiding water loss due to evaporation, runoff and infiltration. It has also been found to raise crop yields significantly. Field trials in Punjab, Pakistan have found the payback period to be one to two years for fruit plants, and three to six years for vegetables [13]. In Tamil Nadu, India, a* ***precision irrigation*** *project has allowed farmers to triple water efficiency while saving on labour; the investments achieved cost recovery within a single season [14].* ***Drip irrigation***[15] *in Israel, which has become its predominant form of irrigation, has led to significant gains in water efficiency and crop yields [15]. In Egypt, drip irrigation has a net return per hectare increase of up to 67% compared to traditional non-drip irrigation [16]. In Mexico, the Livelihoods Fund for Family Farming enable vulnerable farmers to invest in drip irrigation equipment by providing the necessary training, and access to financing. This resulted in a 50% - 70% decrease in water consumption, strengthening the resilience of the city's main aquifer [17].*

Rainwater harvesting systems, *which store rainwater in the soil of non-tilled fields, terraced fields and in small farm tanks at the scale of the micro-watershed and village (e.g. micro-dams and aquifers), provide farmers with a reliable source of water throughout the seasons [18].*

- *Bhungroo, an innovative system to capture and store rainwater in Gujarat, India, during the monsoon season demonstrates the potential efficiencies. Water harvested over just ten days can supply 18,000 marginal farmers with water for as long as seven months. It has increased annual income by three times, with a payback period of three years [19].*

- *In Africa, the use of Zaï pits, or small soil pits dug in fields, is a widespread rainwater or surface runoff harvesting practice that also improves soil health. Organic materials that are placed in the pits*

14 Micro-irrigation consists of drip irrigation systems, subsurface drip irrigation systems, micro spray irrigation systems.
15 Drip irrigation has a field efficiency rate of 90%, which means that 10% of water is not utilised by crops, and is lost to surface runoff, deep percolation, evaporation and transpiration.

attract termites which burrow into the soil and digest organic materials to make nutrients more easily available to crops, thus improving soil health. These pits can concentrate the collection and storage of water up to 500% the soil capacity throughout dry seasons, improving soil fertility and strengthening drought resilience of the fields. Many applications of Zaï pits in Burkina Faso have increased grain yield by 120% [20].

Enhanced rainfed farming is a nature-based system which aims to improve rainfall efficiency by utilising techniques that capture and maintain soil moisture [21]. This includes capturing water to increase its availability through shaping landscapes (e.g terracing), storing water to maintain soil moistures and reduce evaporation (e.g. intercropping, soil covering). These practices have been shown to boost production by up to 24% [22].

Box 4: Diversifying crops and cultivation techniques for water and climate-resilient agriculture.

***Crop switching and use of new seeds** can have major impact on water consumption.*

a. *Studies in India have shown that switching from rice to millet and sorghum in the monsoon season and from wheat to sorghum in winter can reduce water consumption by 32% and increase farmers' profits by 140% [23].*

b. *Life science research has enabled the development of resilient rice varieties that are drought- and flood-tolerant, resistant to disease and can be cultivated with a three-fold reduction of water [24].*[16] *Smallholder farmers can enjoy consistent yields from such rice varieties in the face of climate and water-related stresses.*

c. *A study incorporating data from over 2000 farms across 11 countries have shown that diversifying cultivation practices – such as use of composting and mulching – has led to social and environmental benefits without significant yield losses. In addition, farmers who integrated multiple strategies or practices have experienced comparatively stronger increase in food security [25].*

***Direct Seeding of Rice** (DSR) involves sowing rice seeds directly into the field instead of transplanting seedlings into flooded fields. In the Philippines, its use has saved up to 18% of water [26]. DSR also reduces labour required by up to 24% and has the potential to increase yields by 13 – 18% [27].*

Box 5: Regenerative agriculture for soil health, ecosystem services regeneration, green water and livelihoods.

The core principles of regenerative agriculture are minimizing soil disturbance, entailing no tillage; maintaining soil cover by growing cover crops, leaving crop residues post-harvest, and mulching; and managing crop rotation by incorporating a wider range of crop species.

***Improving soil health.** Regenerative agriculture techniques include no-tillage farming, cover-cropping (where a variety of plants are grown in between cash crops), intercropping (where different are grown together in rows or mixed), agroforestry (where crops are grown in association with trees), and crop rotations (where soil fertility is boosted biologically through the closing of nutrient loops). These techniques can increase soil organic matter, which in turn improves the capacity of soil to hold water, as well as the capacity of plants to take up water [28]. For every 1% increase in soil organic matter, US cropland can store the same amount of water that flows over Niagara Falls over 150 days [29]. Restoring mangroves also helps to prevent the influx of saline water have helped to restore rice paddies, while boosting depleted fish stocks and improving income of farmers [30].*

16 For instance, the rice strain T5105, known as "Temasek Rice", piloted in Banda Aceh and Yogyakarta, has reported a yield twice as high as standard and with a slightly longer growth duration, without compromising grain quality [27].

Ecosystem services regeneration. *Regeneration practices of fostering biodiversity in agriculture such as crop diversification, inoculation of microorganisms into the soil, has been proven to result in win-win support of services and crop yields [31]. Recycling agricultural waste into Biochar have also been proven to improve soil ecosystem services – sequestering carbon for longer duration, improving water holding capacity of soils, and restricting soil pathogen attacks on plants [32].*

Improving crop yields and livelihoods. *Regenerative agriculture also improves the livelihoods of smallholder farmers through its lowered cost, reduced labour, and increased crop yield. Farmers' annual income in Southern Ethiopia is comparatively higher in regenerative agriculture practice than in conventional agriculture practice [33]. OCP, a mineral and fertiliser producer, has also pioneered a mobile soil laboratory which offers farmers a health-check for their soil to determine deficiencies in key macronutrients. With the data, farmers can then obtain a bespoke fertiliser mix, avoiding unnecessary fertiliser use, protecting soils and boosting yields. In Ethiopia, the program has resulted in an increase in yields by 37%, and reduction in fertiliser spending by 20% [34]. Studies on intercropping of soybean with wheat have found that while farmers may experience a decline in profits up to 60%, due to lower crop yields and added cost of seeds and new machinery, they will experience 70% to 120% higher profitability in the long term, with a return on investment of 15% to 25% over 10 years [35]. Proposed crop rotations in the Upper Litani Basin, Lebanon towards high profit, low water usage crops to maximise water and economic productivity has been modelled to reduce blue water use by 20%, and increase profits by 50% [36].*

Other than food crops, regenerative agriculture practices can also be adopted in dairy production. ***The East Africa Dairy Development Programs*** *aims to boost the milk yields and incomes of small-scale farmers in Africa (Kenya, Uganda and Tanzania) so they can lift their communities out of hunger and poverty [37]. The program promotes climate smart and natural resource management practices, aiming to increase farm productivity, and make dairy farmers more resilient to climate change. It promotes the usage of cow dung in production of biogas and compost manure, reducing the need for inorganic fertilisers, and improving soil health. Planting fodder legumes help to improve livestock diets, while improving soil fertility [38]. The* ***Regenerative Cotton Standard*** *(RCS) sets out a voluntary standard for cotton grown by small-scale farmers using regenerative agricultural practices. When working their fields in accordance with the RCS standard, farmers receive support with applying proven cultivation practices, enabling them to increase climate resilience while restoring depleted soils [39].*

Direct investment from large companies can help farmers shift to regenerative agriculture, leading to significant blue water savings. For example, the Livelihoods-Caranuas project, launched by Livelihoods Funds for Family Farming (L3F), Bonafont-Danone and SEBRAE (the Brazilian SMEs development agency), aimed to preserve Tinguá's water resources through sustainable land use. It enabled smallholder farmers to transition to organic farming, while increasing their income by 60%. The project provided farmers with agroecology kits, training in drip irrigation, and strategies to optimise farming and labour resources [40].

Box 6. Enabling conditions to foster greater demand for regenerative agriculture products

As food and beverage businesses increasingly account for the link between nature and business resilience, the demand for regenerative agriculture is growing and transforming entire supply chains [41]. Large agro-industry coalitions are adopting regenerative agriculture practices, and major companies are sourcing these products indirectly through traders and cooperatives. Farmers' cooperatives help address market barriers by developing shared marketplace infrastructure tailored for regenerative agriculture, including processing facilities and distribution networks for sellers [42].

Companies are increasingly aware of supply chain and transition risks, particularly the dangers of lagging in the shift towards a nature-positive economy. As a result, they are becoming less reluctant to pay premiums for regenerative agriculture products, which not only help secure a reliable and sustainable product supply, but also enable suppliers to comply with tighter regulations such as the EU Regulation on Deforestation-Free Products.

For example, Nestle has committed to paying premiums for raw materials produced through regenerative agriculture and to purchasing larger quantities [43]. Similarly, Danone's pricing mechanisms support farmers transitioning to regenerative agriculture practices through premiums or guaranteed margin of costs [44].

To increase resilience and undertake transformation to embed sustainability in their business functions, some companies have focused on portfolio design and conducted frequent portfolio assessments to assess each product's market performance against its environmental performance, and inform decisions on products to push, redesign or phase out.

Box 7: Redirecting subsidies to support water conservation.

Subsidies for conservation. *The Upper Basin System Conservation Pilot in USA is a voluntary, multi-state programme that pays water users to save water [45]. Farms can take advantage of the programme in various ways such as switching to drought resistant crops [45]. In Gujarat, India, a pilot programme that paid farmers for pumping less groundwater than the stipulated benchmark led to those on the programme pumping 24% less time compared to other farmers [46]. While programs that paid farmers for using less electricity for pumping groundwater in Gujarat and Punjab have had mixed results, in several states in India, efficient delivery of subsidies for micro-irrigation technologies has resulted in widespread adoption by hundreds of thousands of farmers [47] [48].*

Targeted subsidies for Alternate Wetting and Drying (AWD). *Directing AWD subsidies at tube well owners who pay to extract water have proven more effective than directing AWD subsidies at farmers who often pay a fixed fee per acre to access water. Farmers in the Mymensingh and Kishoreganj districts of Bangladesh are more than twice as likely to adopt AWD when subsidies are focused on owners of the AWD pipes [49].*

Box 8: Pooling resources for Cluster Farming in Ethiopia, The Philippines, and Vietnam; Irrigation Cooperative in Tanzania; Water Users' Associations in China

Ethiopia. *As agriculture is dominated by subsistence and smallholder farmers, cluster farming is now being promoted as a pathway to improve water efficiency, increase yields and reduce poverty [50]. Farm households each contribute at least 0.25 hectare of land to a cluster. The cluster must be at least 15 hectares to harness the full benefits of participation [50]. Farmers also commit to cultivating crops prioritised by the cluster and adhering to the best farm agronomic recommendations.*

Tanzania. *The Ochuna irrigation scheme is managed by a cooperative in which farmers buy shares [51]. Farmer members pay a fixed price per acre per year to cover the costs of electricity to operate the water pumping station. The cooperative also provides training and loans to farmers, and invests in machinery for producing and transporting rice. These smallholder rice farmers have seen production grow by 70% [51].*

Uganda. *BRAC Uganda, an NGO, runs an Agriculture, Food Security and Livelihood (ASFL) programme to train farmers in climate-smart agriculture and equip them with inputs like seeds, tools, poultry, livestock, to improve their production and livelihood. Microfinancing solutions are also offered to support farmers excluded from mainstream finance to jumpstart their businesses. [52]*

Vietnam. *The Small Farmers, Large Field initiative encourages farmers to integrate multiple small rice areas into one large field. It gives them greater bargaining powers with buyers and input suppliers, and has increased mechanisation [53]. In addition, by transplanting crops at the same time, farmers can utilise improved irrigation and other technologies.*

The Philippines. *Started in 2020, the Farms and Fisheries Clustering and Consolidation (F2C2) Program seeks to advance the interests of small farmers through clustering and consolidation of production, processing and marketing activities [54]. The government is also able to more efficiently channel assistance,*

including ICT services. F2C2 is the first comprehensive and holistic initiative to be implemented at the national level in the Philippines.

China. *In Zhangye, China, farmer members of the Water Users' Association actively optimized cropping systems to save water. They actively reduced cereals, replacing it for high value low water use sweet peppers and tomatoes [55].*

Box 9: Cattle Night Corralling to rehabilitate degraded lands

Uganda. *Regreening the Ugandan cattle corridor*

The Uganda cattle corridor spans a third of Uganda from the southwest to the northern and northeastern borders. Widespread cultivation, overgrazing and charcoal production across the years have led to severe land degradation. Efforts to reseed the degraded pastures were to no avail as soil erosion continued and termites repeatedly consumed the grass seedlings. Taking an idea from Ethiopia, Ugandan Animal Science researchers at the Makerere University convinced cattle keepers to corral their animals together at night to concentrate manure and do so for two weeks before reseeding the pasture. This change in cattle management enabled the reestablishment of grass as the termites preferred manure over grass seedlings. Once grass cover was established, rainfall infiltration into the soil greatly improved, soil moisture was retained, pasture production increased from nothing to about 3000 dry weight kg per hectare and soil erosion stopped.

The use of manure seemed to serve as a trigger to flip the ecosystem back into a more productive and sustainable state of production and secure water in the ecosystem. This prevented surface runoff and sedimentation of water bodies or natural water storage areas. Restoration of upslope vegetative pasture also resulted in reduced surface water runoff and evaporation, prevented sedimentation of valley tanks and enabled maintenance of higher quality and volume of reservoir water. Within the reservoir, research found that water plants such as the Nymphaea and Lemna species allows aeration which increases the efficiency of nitrification and enabled more nitrogen to be made available to the plants and the soil. Furthermore, Lemna species of water plants reduces evaporative water loss up to 20% compared to open water sources. Upon realisation of these research findings, local communities have passed by-laws to protect the riparian vegetation and water quality.

Coupled with restoration of upslope pasture, the transformative management of agroecosystem was able to reverse a non-linear and seemingly irreversible change to the degraded land [56].

Ethiopia. *Rangeland covers close to 65% of Ethiopia's land mass which is taken up primarily for livestock feed. Plant vegetative cover, species composition and biomass yield have been affected by severe land degradation from increase in population, urbanisation, overgrazing and rangeland mismanagement.*

A study using cattle impact tools including trampling, dunging in a concentrated area for short periods of time against a control and concluded that cattle impact tools should be explored for the rehabilitation of degraded rangeland in tropical regions like Ethiopia [57]. The physical action of cattle trampling breaking down soil for greater water infiltration and retention with the application of manure as a source of nutrient flow for plants, have greatly promoted soil seed bank regeneration, vegetation cover, soil fertility, and soil moisture retention. The study found that cattle night corralling had obtained more than 90 times higher biomass in moderately degraded rangeland and about 200 times higher biomass yield in severely degraded rangeland.

Box 10: Innovations to reduce non-revenue water (NRW)

Materials. *A survey of water mains in North America found that ductile iron (5.5 leaks/100 miles/year) and PVC pipes (2.3 leaks/100 miles/year) are vastly less prone to leaks compared to traditional materials such as cast iron (34.8 leaks/100 miles/year) [58].*

Artificial Intelligence and Sensor technologies. *Technologies that are already available enable real-time monitoring of water demand and automatic adjustment of pressure in the water pipes, that in turn limits leakages [59] [60]. Innovations such as acoustic loggers and unused fibre optics cables can detect vibrations from water pipes and significantly reduce the manpower required for leak detection [61]. They can survey large pipe distances, identifying leaks in a much shorter time and identify unreported and background leaks which contribute more to NRW over time [62]. AI solutions have also proven to be a possible affordable and accessible means to reduce NRW. For example, the AI Co-Pilot from Teamsolve analyzes operational data to optimize maintenance schedules, helps troubleshoot system failures more efficiently and facilitates tracking of leaks to ensure they are repaired faster. This can result in a 20% improvement in asset performance and significant savings in both water and operational costs.*

Satellite-based water pipe leakage detection enabled by AI *– The Inter-American Development Bank funded a programme across Argentina, Mexico, Trinidad & Tobago, Brazil and Uruguay to adopt a non-intrusive satellite-based method developed by Asterra to identify and control water loss-detection. The total cost of the programme was only USD $479,000 but yielded USD $32 million in water cost savings, delivering over 70 times return of investments. In one of the projects, the Argentinian utility AySA worked with Asterra to run two pilots in Buenos Aires covering 5,000 km of pipes. The project reported a 128% increase in leak detection efficiency and water savings of 2 million m3 per year (sufficient for 16,700 persons) [63] [64]. The success of the pilot has led to a five-fold expansion of the project.*

Box 11: Manila Water Reduces Non-Revenue Water

Manila Water's approach to reducing non-revenue water puts together a multi-pronged strategy of proactive technical solutions, engineering, and social interventions. Beyond rehabilitating aged infrastructure and conducting swift repairs of leaks, Manila Water had restructured planning areas to smaller, more manageable District Metering Areas (DMAs) and facilitated the implementation of leak detection and pressure management strategies at a localised level [65]. Managers assigned to each DMA are empowered to treat each one as individual business units and meet business targets in an entrepreneurial manner by proposing additional investments to reduce NRW and increase profits through increased billable water. The structure went all the way down to informal street leaders, who helped provide information about pipe bursts, leaks, and water outages [65]. Manila Water also actively built strong community relationships which enabled leak reporting and illegal connections, enabling the utility to act swiftly and reduce water loss, while fostering a sense of accountability within the community [66].

Manila Water also implemented a social programme called Tubig Para Sa Barangay which aims to provide new, affordable and safe water connections to low-income and marginalised communities. By 2023, the programme has benefitted close to 2 million residents through more than 750 projects [66].

Box 12: Municipal potable reuse of treated wastewater.

*Windhoek, **Namibia** has been implementing direct potable reuse since 1968, which accounts for approximately 25% of their drinking water supply. Further expansion of their water reclamation plants aims to increase the supply of drinking water from reclaimed water to 50% [67].*

*The Maynilad facility in Manila, **Philippines** operationalised a reclamation facility in Oct 2023, providing potable water through a direct potable reuse process. The facility provides at least 10 million liters of water per day to two barangays (or districts), serving over 38,000 customers.*

*Orange County Water District in **California** runs the world's largest water purification system for indirect potable reuse[17] through its Groundwater Replenishment System. It is set to grow further – ongoing expansion will increase its supply capacity from 100 to 130 million gallons of water per day (an increase from serving 850,000 people to 1 million people). California has gone further to approve regulations for direct potable reuse in Dec 2023, paving the way for a USD $6 billion direct potable reuse facility in Carson [68].*

***Singapore's** NEWater process recycles treated used water into ultra-clean, high-grade reclaimed water, meeting about 20% of water demand today through direct non-potable use by industrial customers. During dry periods, NEWater is also added to reservoirs to blend with raw water which is then treated at the waterworks, enabling indirect potable reuse.*

Box 13: Fit-for-purpose on-site water usage in urban settings

***San Francisco** has strengthened mandatory rules for all new buildings with footprints larger than 100,000 square feet to include on-site water reuse systems to reduce the use of potable water [84].*

*In **Singapore,** harvested rainwater in public housing estates is minimally treated for washing of common areas and irrigation of gardens and parks. Adopting fit-for-purpose water leads to a reduction in potable water use of more than 50% [69]*

*In **Bengaluru, India,** there are multiple initiatives that have been undertaken to reuse treated water. More than half of treated wastewater is being reused for a range of uses by industrial parks and manufacturing firms, for watering public parks and golf courses and for heating and cooling power plants. In addition, Koramanagala-Challaghatta valley tank-filling lift-irrigation project, pumps secondary treated wastewater from Bengaluru city's five sewage treatment plants for storage in rain-fed tanks to be used for agriculture and animal husbandry, and recharging groundwater [70].*

Box 14: Reuse of wastewater in industrial reuse.

***Industrial reuse.** The water-intensive wafer fabrication sector can now achieve high water recycling rates in a cost-effective manner by reusing reject streams from ultra-pure water production for cooling. Leading wafer fabrication plants in Taiwan operate at above 80% recycling rates. Process water in semiconductor manufacturing can also be purified and reused in manufacturing processes, to reduce overall water usage. Amkor Technology has been utilising reverse osmosis and electro-deionisation systems together to purify and re-use process water, resulting in a 12% decrease in water withdraw intensity in 2022 [71].*

Since 2015, Tampa Electric has utilised treated wastewater from nearby cities for cooling at the Polk Power Station, minimising withdrawals of groundwater. It also reduces the discharge of wastewater into Tampa Bay, improving the biodiversity of the Bay [72].

***Agricultural reuse.** The reuse of wastewater (treated and non-treated) for irrigation is already widespread, particularly in arid and semi-arid countries such as Australia, Israel and Egypt.*

Egypt has been reusing nutrient-rich agricultural drainage water (which includes a blend of treated domestic and agricultural wastewater) to sustain agricultural activities. An ongoing SafeAgroMENA project seeks to help ensure the sustainability of such practices, especially for small-scale farmers, amidst health concerns of emerging contaminants from illegal discharges in Egypt. [73]

17 Indirect portable reuse introduces purified water into an environmental buffer (e.g., a groundwater aquifer or a surface water reservoir, lake, or river) before the blended water is treated at a water treatment plant and piped to the consumer.

Box 15: Innovations in industrial water use

Data centres. *There are ongoing demonstration projects which reduce water use in data centres. Google's data centre in Belgium does away with chillers. It instead utilises outside air to keep temperatures down; if temperatures are too high, Google shifts the compute loads to other facilities [74]. Meta has conducted studies in order to design and operate data centres at an optimal relative humidity, temperature and airflow, achieving water savings of 40% over 9 months. Meta's data centres are on average 80% more water-efficient than the average data centre [75]. Efforts should be made to utilise water that does not have competing uses for data centres, such as seawater. Google's data centre in Hamina, Finland, utilises seawater from the Bay of Finland in its cooling system, thus reducing energy use [76]. Equinix, a vendor-neutral data centre provider, aims to increase the efficiency of its cooling water by controlling the pH level of cooling water and utilising mechanical filtration to remove solids and limit turbidity [77].*

Semiconductor manufacturing. *Using sprays to rinse wafers instead of baths to remove impurities has been shown to reduce water usage and total rinse times without sacrificing wafer cleanliness. Efforts are also being made to replace wet with dry processes where possible (e.g. anisotropic etching with dry plasma etches instead of wet isotropic etches) [78].*

Box 16: Demonstration of Affordable Community Level Water Treatment Systems.

India. Rite Water Solutions *provide decentralised water purification systems, solar-powered water treatment units and mobile water ATMs, as part of the Jal Jeevan Mission to provide clean drinking water to India's rural population [79]. The water purification generates chlorine onsite from common salt, without chemicals, allowing it to be easily applied to any village without the need for chemicals which are difficult to procure [79].*

The ***Tamil Nadu Urban Sanitation Support Program*** *(launched in 2016) seeks to scale urban sanitation through decentralised sanitation systems to an urban population of over 35 million by ensuring safe collection of sewage from on-site septic tanks and more water-efficient treatment in decentralised plants. This prevents the unsafe disposal of faecal sludge into waterbodies around cities which contaminates drinking water sources. [80] With an investment of USD $30 million, the programme already delivers services to 11 million people through decentralised systems spanning both rural and urban areas, and will deliver to another 6 million in the coming year, with additional public investments. This makes it more cost-effective than conventional networked sewerage both as a stand-alone and as a complementary system.*

Ha Tinh Province, Vietnam. *Decentralised water treatment systems fitted with membranes consisting of new carbon nanoparticles are being utilised to provide 30,000 people with clean water. The membranes are manufactured without use of solvents, are much less costly and more environmentally friendly, and require less cleaning [81]. Each system costs USD $500,000 to $600,000 to build, much lower than conventional systems. They are also able to treat high turbidity water effectively, eliminating the need for chemical pre-treatment, resulting in both significant operational cost savings and vastly less sludge and contamination of water bodies [82].*

Hlaing Thar Yar, Myanmar. *A Reverse Osmosis (RO) water treatment system was installed to treat polluted saline groundwater and provide clean drinking water to community of 1500 people [83]. This project was implemented by Nanyang Technological University's NEWRIComm. The system addresses traditional concerns over RO systems which have been energy-intensive and expensive [83]. Efforts to address this have yielded estimated cost of 30% savings[18] over 5 years, opposed to a tradition RO system. Efforts included the integration of instruments for continuous monitoring at critical process stages, which were selected for their simplicity, ease of maintenance and affordability. Internet of Things protocol was also introduced to allow for remote monitoring of the process and providing guiding support for on-site operators.*

18 These included the integration of instrumentation for continuous monitoring at critical process stages, which were selected for their simplicity, ease of maintenance and affordability. Internet of Things protocol was also introduced to allow for remote monitoring of the process, allowing on-site operators to be guided.

Tanzania. *A solar irrigation project by Climate Action Network Tanzania had installed six solar powered pumps to increase the crop yield of smallholder farmers by at least 50%, while also enabling a POU water treatment system to deliver safe water for consumptive and other uses [84]. Unlike advanced water treatment technologies, these low cost POU systems rely on mature technology (such as chemical-based coagulation and membrane-based filtration to remove waterborne pathogens [85].*

France. *As an alternative to costly sewer network provision in sparsely populated areas, French municipalities turn instead to off-the-grid sanitation solutions implemented by buildings and homeowners to ensure appropriate environmental protection. Through SPANC (the public non-collective sanitation service), the municipality regulates the design and implementation of these off-grid solutions and monitors the proper operation and maintenance of existing installations. Fees for regular inspection are billed to the owner, along with optional maintenance services provided by SPANC [86].*

Box 17: Chlorine-based water treatment solutions

Diarrheal disease due to microbiologically contaminated water is a leading cause of child mortality. Simple, chlorine-based water treatment is inexpensive, widely available, and highly effective against most pathogens. A meta-analysis of 18 randomized evaluations finds that various such treatments averts one in four child deaths, making it one of the most cost-effective health investments available, with estimates of USD 3,000 - $5,000 per death averted [87]

Chlorination is inexpensive and free delivery does not lead to overuse, meaning that long-term public subsidy is highly cost-effective, particularly for programmes aimed at pregnant women and young children. [88]

In settings where central water treatment is not reliable or not yet feasible, interim solutions for water treatment are available. In piped water systems with intermittent flow, water can be treated using passive chlorination; devices are available, appropriate for various types of water source.

In settings where piped water will not be available for some time, point-of-use water treatment, such as bottles of dilute chlorine solution, can be delivered for free during routine maternal and child health visits [89]. Free delivery for pregnant women and young children substantially increases take-up of water treatment.

Box 18: Small-scale desalination for coastal communities

Solar powered desalination has been deployed to benefit 270 households in Dinagat town in the Philippines. This technology will solve the challenge of supplying potable and safe water in areas hit by natural disasters [90].

Engineers from MIT and China have designed a small-scale, passive solar desalination system that is able to produce water at record-high efficiencies at low production cost. The system has water circulating in swirling eddies, similar to oceanic thermohaline circulation [91]. The heat from sunlight causes water in these circulating eddies to evaporate, leaving the salt behind. The water vapour is then condensed into pure drinking water, while the residual salt is expelled. Its long lifespan and lack of reliance on electricity allows for its overall operation cost to be kept low and is estimated to be cheaper than producing tap water in the USA [91].

Box 19: Transforming utility regulation.

Colombia. *While Colombia had achieved extensive coverage for urban sewerage and drinking water, it experiences gaps that affects its poorest inhabitants. The government's differentiated schemes introduced in 2017 permits utilities to provide water and sanitation services to meet differentiated regulatory targets depending on the segment of market it serves, while eventually complying fully with general sector regulations by the end of the scheme. For example, for sewage, utilities can use alternative methods from public pipes and non-conventional sewage systems such as septic tanks or latrines. This has enabled the utilities to reach the underserved more quickly, and progress towards common service standards [92] [93].*

Brazil. *The Brazilian water market is a successful example of using long-term concessions (30 – 35 years) to get private sector firms to transform poorly managed municipal water utilities [94]. The focus of concession auctions has been to expand coverage in poorer areas, improve quality of service and reduce environmental impact. Subsidised formal connections have replaced illegal tapping. Tariffs are fixed, with inflation adjustments only. Once awarded, the tariff is no longer subject to periodic regulatory reviews but is fixed for the whole concession period (except for the allowed annual inflation adjustment). This provides certainty to the bidder on what returns to expect during the life of the concession based on its business plan. Private investors capture full upside from cost cutting and other efficiency improvements. As such, the concession is incentivised to invest to deliver the pre-agreed service levels and ensure continuous improvements.*

Box 20: Financing decentralised systems

Uganda's direct transfer of resources to local authorities. *The provision of water services in refugee settlements in Uganda was highly fragmented, and posed significant financial and capacity pressure on humanitarian support. The transfer of water systems in refugee settlements in Uganda from humanitarian systems to national water authorities enabled better coordination and long-term sustainability of water services. Select refugee settlements were posed nominal water user fees to introduce refugees to a fee-based system and to build a financially sustainable system eventually. A joint sector review for water and sanitation in Uganda has also explored a dedicated, integrated budget line for sanitation and hygiene to overcome the issue of lack of priority for grants into water and sanitation [95].*

Telegana, India *provides an example of funding decentralised systems through fee collection from users. Locally owned and operated water purification systems, called iJal stations, have provided safe and clean drinking water to over 100,000 people [96]. Users pay an affordable fee for the water from these community operated stations, which supports operating costs. After covering OPEX costs, the revenues are shared among the individual or group managing the station, regular service fee payments and the sustainability fund. The usage of these stations is also regularly monitored, and stations relocated if needed to optimise asset utilisation and financial management [97].*

References

[1] **B. Bouman and T. Tuong,** "Field water management to save water and increase its productivity in irrigated lowland rice," *Agriculture Water Management,* vol. 49, no. 1, pp. 11-30, 2001.

[2] **ADB,** "Climate-Smart Practices for Intensive Rice-Based Systems In Bangladesh, Cambodia, and Nepal," Manila, Philippines, 2019.

[3] **R. M. Lampayan, R. M. Rejesus , G. R. Singleton and B. A. Bouman,** "Adoption and economics of alternate wetting and drying water management for irrigated lowland rice," *Field Crop Research,* vol. 170, pp. 95-108, 2015.

[4] **M. Ishfaq, N. Akbar, A. S. Anjum and M. Anwar-Ijl-Hao,** "Growth, yield and water productivity of dry direct seeded rice and transplanted aromatic rice under different irrigation management regimes," *Journal of Integrative Agriculture,* vol. 19, no. 11, pp. 2656-2673, 2020.

[5] **A. Kumar and M. Katagami,** "Developing and Disseminating Water-Saving Rice Technologies in Asia," 2016.

[6] **World Business Council for Sustainable Development,** "Deep dive: Rice production in the Mekong Delta, Vietnam," WBCSD, 2023.

[7] **World Wildlife Fund,** "WWF DFCD seals groundbreaking partnership to reverse degradation of Mekong Delta," WWF, 02 August 2021. [Online]. Available: https://vietnam.panda.org/en/?369235/WWF-DFCD-seals-groundbreaking-partnership-to-reverse-degradation-of-Mekong-Delta.

[8] **S. Gupta, V. Mann, J. Mazzucotelli, M. Gomez and H. Maqsood,** "Vietnamese rice farmers go high-tech to anticipate a low-water future," 24 July 2023. [Online]. Available: https://news.mongabay.com/2023/07/vietnamese-rice-farmers-go-high-tech-to-anticipate-a-low-water-future/.

[9] **T. M. Nestor, A. Melchizedek, B. V. Jezy, S. Eunice and T. L. Jean,** "Agrinex: A low-cost wireless mesh-based smart irrigation system," *Measurement,* vol. 161, 2020.

[10] PRNewswire, "DataYoo Revolutionizes Precision Agriculture with AI," 4 July 2024. [Online].

[11] **FarmiSpace,** "Make Agricultural Decisions and Digitize Field Management with Satellite Data for Just USD 0.12 a Day," 26 June 2024. [Online]. Available: https://farmispace.datayoo.com.tw/article/9ddc93de-f993-40d4-bac6-c32b8633adf8.

[12] **IWMI,** "Phone app gives opportunity to improve water productivity in Lebanon," 21 April 2020. [Online]. Available: https://www.iwmi.cgiar.org/blogs/phone-app-gives-opportunity-to-improve-water-productivity-in-lebanon/.

[13] **M. Aziz, S. A. Rizvi, M. A. Iqbal, S. Syed, M. Ahraf, S. Anwer, M. Usman, N. Tahir, A. Khan, S. Asghar and J. Akhtar,** "A Sustainable Irrigation System for Small Landholdings of Rainfed Punjab, Pakistan," *Sustainability ,* vol. 13, no. 20, 2021.

[14] **A. Velkar,** "Tamil Nadu Precision Farming Project: An Evaluation," 2008.

[15] **C. Perry,** "Does improved irrigation technology save water?," 2017.

[16] **A. Abdelrahman,** X. Chunping , J. Cheng and F. Muhammad, "Investment profitability and economic efficiency of the drip irrigation system: Evidence from Egypt," *Irrigation and Drainage ,* 2010.

[17] **Livelihood Funds,** "Livelihood Funds for Family Farming," [Online]. Available: https://livelihoods.eu/l3f/.

[18] **The World Bank,** "What the Future Has in Store : A New Paradigm for Water Storage," 2023.

[19] **United Nations Climate Change,** "Bhungroo | India," [Online]. Available: https://unfccc.int/climate-action/momentum-for-change/women-for-results/bhungroo.

[20] **CGIAR,** "Water for Dry Land Farming with Zai".

[21] **Danone,** "Acknowledge Enchanced Rainfed Farming to Foster Sustainable Food Systems While A Global Water Crisis," 2024.

[22] FAO, "Overcoming water challenges in agriculture," [Online]. Available: https://www.fao.org/interactive/state-of-food-agriculture/2020/en/.

[23] Ruparati Chakraborti , K. F. Davis, R. Defries, N. D. Rao, J. Joseph and S. Ghosh, "Crop switching for water sustainability inIndia'sfood bowl yields co-benefits for foodsecurity and farmers' profits," *Nature Water,* Vols. 864 - 878, no. 1, 2023.

[24] Y. Luo and Z. Yin, "Marker-assisted breeding of Thai fragrance rice for semi-dwarf phenotype, submergence tolerance and disease resistance to rice blast," *Molecular Breeding* , vol. 32, no. 3, 2013.

[25] L. V. Rasmussen, I. Grass, Z. Mehrabi, O. Smith, R. Bezner-Kerr, J. Blesh, L. A. Garibaldi, E. M. Isaac, C. M. Kennedy, H. Wittman, P. Batary, D. Buchori, R. Cerda, J. Chara, D. W. Crowder, K. Darras, K. Demaster, K. Garcia, M. Gomez, D. Gonthier, P. Hidyat, J. Hipolito, M. Hirons, L. Hoey, D. James, I. John, A. D. Jones, D. S. Karp, Y. Kebede, C. B. Kerr, S. Klassen, M. Kotowksa, H. Kreft, R. Llanque, C. Levers, D. J. Lizcano, A. Lu, S. Madsen, R. N. Marques, P. B. Martins, A. Melo, H. Nyantakyi-Frimpong, E. M. Olimpi, J. P. Owen, M. Qaim, S. Redlich, C. Scherber, A. R. Sciligo, S. Snapp, W. E. Snyder, I. Steffan-Dewenter, A. E. Stratton, J. M. Taylor, T. Tscharntke, V. Valencia, C. Vogel and C. Kremen, "Joint environmental and social benefits from diversified agriculture," *Science,* vol. 394, no. 6691, pp. 87-93, 2024.

[26] A. Chaudhary, V. Venkatramanan, A. K. Mishra and S. Sharma, "Agronomic and Environmental Determinants of Direct Seeded Rice in South Asia," *Circular Economy and Sustainability,* pp. 253-290, 2023.

[27] M. Mallareddy , R. Thirumalaikumar, P. Balasubramanian, R. Naseeruddin , N. Nithya , A. Mariadoss, N. Eazhilkrishna, A. K. Choudhary, M. Deiveegan , E. Subramanian, B. Padmaja and S. Vijayakumar, "Maximizing Water Use Efficiency in Rice Farming: A Comprehensive Review of Innovative Irrigation Management Technologies," *Water,* vol. 15, no. 10, 2023.

[28] A. M. Abdallah, H. S. Jat, M. Choudhary, E. F. Abdelaty, P. C. Sharma and M. L. Jat, "Conservation Agriculture Effects on Soil Water HoldingCapacity and Water-Saving Varied with Management Practicesand Agroecological Conditions: A Revie," *Agronomy,* vol. 11, p. 1681, 2021.

[29] L. Bryant, "Organic Matter Can Improve Your Soil's Water Holding Capacity," May 27 2015. [Online]. Available: https://www.nrdc.org/bio/lara-bryant/organic-matter-can-improve-your-soils-water-holding-capacity.

[30] Livelihood Funds, "Senegal: The largest mangrove restoration programme in the world," [Online]. Available: https://livelihoods.eu/portfolio/oceanium-senegal/.

[31] G. Tamburini, R. Bommarco, T. C. Wanger, C. Kremen, M. G. V. Heljden, M. Liebman and S. Hallin, "Agricultural diversification promotes multiple ecosystem services without compromising yield," *Science Advances,* vol. 6, no. 45, 2020.

[32] M. Gopal, A. Gupta, S. K. Hameed, N. Sathyaseelan, T. K. Rajeela and G. V. Thomas, "Biochars produced from coconut palm biomass residues can aidregenerative agriculture by improving soil properties and plant yieldin humid tropics," *Biochar,* pp. 211 - 266, 2020.

[33] T. A. Gebeyehu, "Adoption and impacts of conservation agriculture on smallholder farmers' livelihoods in the case of Arba Minch Zuria district of Southern Ethiopia," *Cogent Social Science,* vol. 9, no. 1, 2023.

[34] S. Savage, "Can Africa one day help feed the world's growing population?," 3 April 2024. [Online]. Available: https://www.ft.com/content/99958fff-8f69-42ca-b90b-5e2e2677845b.

[35] J. Bugas, H. Conant, S. Hoo, F. Bellino, S. Unnikrishhnan and M. Westerlund, "Making Regenerative Agriculture Profitable for US Farmers," 15 August 2023. [Online]. Available: https://www.bcg.com/publications/2023/regenerative-agriculture-profitability-us-farmers.

[36] H. Nouri, B. Stokvis, S. Chavoshi Borujeni, A. Galindo, M. Bruganch, M. Blatchford, S. Alaghmand and A. Hoekstra, "Reduce blue water scarcity and increase nutritional and economic water productivity through changing the cropping pattern in a catchment," *Journal of Hydrology,* vol. 588, 2020.

[37] World Agroforestry, "East Africa Dairy Development Program," [Online]. Available: https://www.worldagroforestry.org/project/east-africa-dairy-development-program.

[38] weADAPT, "Climate-smart agriculture put into practice in smallholder dairy development project in Kenya," 11 December 2012. [Online]. Available: https://weadapt.org/knowledge-base/climate-food-security-and-agriculture/climate-smart-agriculture-put-into-practice-in-smallholder-dairy-development-project-in-kenya/.

[39] Regenerative Cotton Standard, "Regenerative Cotton Standard," [Online]. Available: https://regenerative-cotton.org/en/home/.

[40] Livelihoods Fund, "Water preservation and fight against poverty: Livelihoods' Bet in Rio," 20 June 2019. [Online]. Available: https://livelihoods.eu/water-preservation-fight-poverty-livelihoods-rio/.

[41] C. G. S. V. A. &. M. A. Bande, "Climate progress is stalling in the food and beverage industry. Could nature be the solution?," Quantis Insights., 17 July 2024. [Online]. Available: https://quantis.com/news/food-and-beverage-climate-nature-strategy/.

[42] Forum for the Future, "From conventional supply channels to Regenerative Value Networks: A new model for a regenerative marketplace," 2023.

[43] Nestle, "Nestlé unveils plans to support the transition to a regenerative food system," 16 September 2021. [Online]. Available: https://www.nestle.com/media/pressreleases/allpressreleases/support-transition-regenerative-food-system.

[44] K. Askew, "Danone talks regenerative agriculture: Linking dairy and plant-based at farm level can yield sustainability gains," 24 August 2021. [Online]. Available: https://www.foodnavigator.com/Article/2021/08/24/Danone-talks-regenerative-agriculture-Linking-dairy-and-plant-based-at-a-farm-level-can-yield-sustainability-gains.

[45] S. Mullane, "Dozens of Colorado farmers, ranchers and one city offer to cut Colorado River water use in exchange for $8.7M," The Colorado Sun, 13 Feburary 2024. [Online]. Available: https://coloradosun.com/2024/02/13/farmers-city-colorado-river-conservation-program-big-payouts/.

[46] N. Hagerty and A. Zucker, "How farmers in India can be incentivised to save water," 5 June 2024. [Online]. Available: https://www.theigc.org/blogs/climate-priorities-developing-countries/how-farmers-india-can-be-incentivised-save-water.

[47] R. Fishman, L. Upmanu, V. Modi and N. Parekh, "Can Electricity Pricing Save India's Groundwater?Field Evidence from a Novel Policy Mechanismin Gujarat," *Journal of the Association of Environmental and Resource Economists,* pp. 819-855, 2016.

[48] M. Archisman , R. Brouwer and S. Balasubramanya, "Can cash incentives modify groundwater pumping behaviors? Evidence from an experiment in Punjab," *American Journal of Agricultural Economics,* vol. 105, no. 3, pp. 861-887, 2023.

[49] H. Bhandari, U. Chakravorty and M. A. Habib, "Targeted Subsidies for Water Conservation in Smallholder Agriculture," 2022.

[50] G. G. Dureti, M. P. J. Tabe-Ojong and E. Owusu-Sekyere, "The new normal? Cluster farming and smallholdercommercialization in Ethiopia," *Agriculture Economics,* 5 July 2023.

[51] C.-h. Zhang, W. A. Benjamin and M. Wang, "The contribution of cooperative irrigation scheme to poverty," *Journal of Integrative Agriculture,* vol. 20, no. 4, pp. 953-963, 2021.

[52] BRAC, "BRAC Uganda Fact Sheet 2017," [Online]. Available: https:www.brac.net/images/factsheet/december17/Uganda-31.12.2017.pdf. [Accessed 3 September 2024].

[53] The World Bank, "Realizing Scale inSmallholder-Based Agriculture," 2021.

[54] Department of Agriculture, "DA kickstarts farm consolidation, clustering program," 12 August 2020. [Online]. Available: https://www.da.gov.ph/da-kickstarts-farm-consolidation-clustering-program/.

[55] Q. Chai, Y. Gan, N. C. Turner, R.-Z. Zhang, C. Yang, Y. Niu and K. H. Siddique, "Chapter Two - Water-Saving Innovations in Chinese

Agriculture," *Advances in Agronomy,* pp. 149-201, 2014.

[56] J. F. M. F. C. L. M. B. J. E. E. G. L. H. J. H. H. a. P.-W. C. Rockström, in *Water resilience for human prosperity*, Cambridge University Press, 2014, pp. 84-85.

[57] D. H. a. K. G. Meskel, "Impact of cattle night corralling on soil properties and vegetation in the semiarid degraded rangeland of Ethiopia.," *Bangladesh Journal of Animal Science,* vol. 51, no. 4, pp. 152-162, 2022.

[58] S. Folkman, "Water Main Break Rates in the USA and Canada: A Comprehensive Study," Utah State University, 2018.

[59] R. Holland, "Doubling down on improving water resilience," Business Times, 5 June 2024. [Online].

[60] G. A. Gericke and R. Kuriakose, "IoT Water Monitor Implementation Strategy," *Journal of Physics: Conference Series.*

[61] Norsar, "Detecting Water Leaks with Fiber Technology," [Online]. Available: https://www.norsar.no/in-focus/detecting-water-leaks-with-fiber-technology.

[62] G. W. Z. B. M. G. A. I. S. S. Malcolm Farley, "The Manager's Non-Revenue Water Handbook," 2008.

[63] "INTERSESSIONAL PANEL OF THE UNITED NATIONS COMMISSIONON SCIENCE AND TECHNOLOGY FOR DEVELOPMENT (CSTD," Geneva, Switzerland, 2022.

[64] ASTERRA, "Satellite-based leak detection saves over $32M in five countries, leading to new three-year contract," 12 October 2023. [Online]. Available: https://asterra.io/resources/asterra-brings-staggering-70x-roi-and-climate-impact-in-latam/.

[65] R. Frauendorfer and R. Liemberger, "The issues and challenges of reducing non-revenue water," Asian Development Bank, Philippines, 2010.

[66] Aqua Tech, "Manila Water Surpasses Global Benchmarks in Water Loss Reduction," 31 July 2023. [Online]. Available: https://www.aquatechtrade.com/news/utilities/manila-water-benchmarks-water-loss-reduction.

[67] Aqua Tech, "DIRECT POTABLE REUSE: NAMIBIA'S FLAGSHIP SUCCESS LEADS TO SECOND PROJECT," 1 February 2023. [Online]. Available: https://www.aquatechtrade.com/news/water-reuse/namibia-second-direct-potable-reuse-project.

[68] I. James, "California prepares to transform sewage into pure drinking water under new rules," 17 December 2023. [Online]. Available: /https://www.latimes.com/environment/story/2023-12-17/california-sewage-potable-reuse.

[69] MND-HDB, "Joint MND-HDB Press Release: Rejuvenating and Greening HDB Towns for Sustainable Living," March 4 2020. [Online]. Available: https://www.hdb.gov.sg/cs/infoweb/about-us/news-and-publications/press-releases/joint-mnd-hdb-press-release-rejuvenating-and-greening-hdb-towns.

[70] P. Earth, "About KC Valley Project," 14 August 2023. [Online]. Available: https://paani.earth/regions/bengaluru_homepage/koramangala-challaghatta-watershed-homepage/kc-valley-project-homepage/kc-valley-project/.

[71] "Water Reduction and Reclamation in PCB Manufacturing," 4 June 2024. [Online]. Available: https://resources.altium.com/p/water-reduction-and-reclamation-pcb-manufacturing.

[72] Tampa Electricy, "Innovative reclaimed water project is "essentially complete" at Polk Plant," 20 December 2017. [Online]. Available: https://www.tampaelectric.com/mediacenter/2017/Innovative-reclaimed-water-project-is-essentially-complete-at-Polk-Plant/.

[73] IHE Delft Water and Development Partnership Programme, "Reuse of nutrient-rich wastewater for a food self-sufficieny in MENA," 2022. [Online]. Available: https://safeagromena.blogspot.com/2022/11/what-is-safeagromena-project.html. [Accessed 2023].

[74] C. Metz, "Google data center born without chillers," 16 July 2009. [Online]. Available: https://www.theregister.com/2009/07/16/google_chillerless_data_center/.

[75] Meta, "Public Water Reporting: Expanding the Operating Envelope," 2016.

[76] Google, "Hamina, Finland," [Online]. Available: https://www.google.com/about/datacenters/locations/hamina/.

[77] Equinix, "Equinix Water Programs," 2024.

[78] PUB, Singapore's National Water Agency, "Best Practice Guide in Water Efficiency - Wafer Fabrication and Semiconductor Sector Version 2," Singapore, 2022.

[79] S. Mani, "This Engineer's Solution Delivers Over 10 Million Litres of Clean Drinking Water Every Day," The Better India, 24 June 2024. [Online]. Available: https://thebetterindia.com/353376/abhijeet-gan-rite-water-solutions-million-litres-clean-drinking-water-jal-jeevan-mission-maharashtra/.

[80] M. Vijendra, S. Sudhakar, M. Anneka and S. Yaseen, "Cluster Approach for Used Water Treatment: A case study," Indian Institue for Human Settlements , 2022.

[81] C. Tan, "S'pore researchers develop affordable large-scale water treatment system for developing nations," 3 October 2023. [Online]. Available: https://www.straitstimes.com/singapore/s-pore-researchers-make-large-scale-water-treatment-affordable-for-developing-nations.

[82] Atera Water, "Revolutionising Sustainable Filtration With TeraStream™," [Online]. Available: https://www.aterawater.com/terastream/.

[83] V. S. T. Sim, "Flowing Towards a Sustainable and Resilient Infrastructural Future," 19 Feburary 2019. [Online]. Available: https://prostruct.com.sg/perspective/flowing-towards-a-sustainable-and-resilient-infrastructural-future/.

[84] Green People's Energy for Africa, "Solar Water Pumps Secure Harvests and Livelihoods," [Online]. Available: Solar Water Pumps Secure Harvests and Livelihoods.

[85] K. P. Ching and H. Y. Ng, "Review of low-cost point-of-use water treatment systems for developing communities," *Clean Water,* 2018.

[86] Public Service France, "Sanitation of domestic wastewater," 22 7 2022. [Online]. Available: https://www.service-public.fr/particuliers/vosdroits/F447?lang=en. [Accessed 11 6 2024].

[87] M. Kremer, S. Luby, R. Maertens, B. Tan and W. Wiecek, "Water treatment and child mortality: A meta-analysis and cost-effectiveness analysis.," 2023.

[88] P. Dupas, B. Nhlema, Z. Wagner, A. Wolf and E. Wore, "Expanding Access to Clean Water for the Rural Poor: Experimental Evidence from Malawi," *American Economic Journal: Economic Policy,* vol. 15, no. 1, pp. 272-305, 2023.

[89] P. Dupas, V. Hoffman, M. Kremer and A. P. Zwane, "Targeting health subsidies through a nonprice mechanism: A randomized controlled trial in Kenya," *Science,* vol. 353, no. 6302, pp. 889-895, 2016.

[90] P. Chandak, "Philippines Launches Solar-Powered Desalination Equipment," 11 February 2022. [Online]. Available: https://solarquarter.com/2022/02/11/philippines-launch-solar-powered-desalination-equipment/.

[91] E. Ralls, "Cheap and drinkable water from desalination is finally a reality," 10 February 2023. [Online]. Available: https://www.earth.com/news/cheap-and-drinkable-water-from-desalination-is-finally-a-reality/.

[92] D. Polaníai, "Water and sanitation for the poorest communities in Colombia's cities," 2022.

[93] D. Polanía, "Colombia's emerging regulatory framework for inclusive sanitation access," 23 August 2021. [Online]. Available: https://thesourcemagazine.org/colombias-emerging-regulatory-framework-for-inclusive-sanitation-access/.

[94] Netherlands Enterprise Agenc, "Business in Brazil's New Sanitation Framework," 2023.

[95] WaterAid, "Think local, act local - Effective financing of local governments to provide water and sanitation services".

[96] Safe Water Network, "Expansion of Safe Drinking Water "iJal Stations' in Telangana: Cost-effective, Replicable, Sustainable Service Delivery".

[97] Safe Water Network, "Relocation of iJal Stations for Asset Protection," 2020.

Appendix 9.1

Data as a foundation for action

Box 1: Examples of companies engaging in water footprint accounting

- **Olam**, *a global food and agri-business, provides detailed Natural Capital accounts [1]. It employs a multi-capital accounting (MCA) approach, following frameworks such as the Natural, Social, and Human Capital Protocols issued by the Capitals Coalition. Its subsidiary, OFI, a food ingredients supplier, employs a shadow price methodology to estimate the societal cost of water consumption, considering variables such as basin water stress and population size. This approach is applied at both the farmer group and processing facility levels, accounting for differing sources and prices of water use. By utilising the Total Economic Value (TEV) framework, OFI reports the various benefits that water provides, beyond market value reflected in municipal water bills.*

- **United Utilities**, *the water company responsible for water and wastewater services in the North West of England, commissioned a North West Regional Natural Capital Account in 2021. In 2024, they published their first Corporate Natural Capital Account which captured key benefits from the natural assets on land that they own, and the costs associated with maintaining them. The company stated that this account would influence their priorities in investments and will feed into their annual TNFD disclosure reporting [2]. The Corporate Natural Capital Account 2023 states that the balance sheet shows significant returns to the utility from natural capital assets equating to £6.6 billion over 60 years, which is driven by the gross value of water supply (£6.3 billion).*

- **Pepsi-Co** *publishes water-related data such as global water use, total water withdrawals, and wastewater discharge in its operations, and the progress being made towards its water goals, such as achieving net positive water impact by 2030, and a 25% improvement in water use efficiency by 2025 [3]. The company takes water into consideration in deciding on the viability of its operations in certain locations. This has led in some instances of them closing plants where lack of water availability and the resulting environmental, social, and financial impacts have outweighed the business benefit of keeping a manufacturing site open [4].*

- **Ford Motor Company**'*s proactive approach to water risk disclosure has positioned them as a sustainability leader in the automotive industry. Ford tracks and discloses water in its direct operations, and has worked with suppliers to set "withdrawal reduction targets" throughout its supply chain [5].*

Box 2: Examples of valuing water as natural capital

- *The Asian Infrastructure Investment Bank (AIIB) is collaborating with the Chinese government on a natural capital project in Inner Mongolia, specifically in Ulanhot City. The project, with a proposed funding of USD 250 million, aims to harvest rainwater to improve groundwater level, ecologically restore the Tao'er River and its wetlands, and support ecological treatment of abandoned quarries. Modelling has shown that the project will result in ecosystem services 11% higher than the baseline, with water provisioning services increasing by 30% [6].*

- *New York City's Catskill Watershed: Payments for ecosystem services (PES) for watershed conservation (beneficiary pays principle) is an emerging market, which remains dominated by the public sector today. The key to unlocking commercial investments in natural capital is to demonstrate a clear link between the investment in upstream supply and downstream benefits for downstream users.*

- *The investment in New York City's Catskill Watershed demonstrates the benefits of leveraging natural ecosystem services for water filtration and storage, thus avoiding the need for costlier water infrastructure. The city invested USD 1 billion to reinforce and expand a host of programmes that protect watershed land surrounding the reservoirs that supply unfiltered drinking water. These include maintaining and upgrading wastewater treatment plants and septic systems, reducing pollution from working farms, managing forests to make room for young trees that absorb more nutrients from precipitation, flood mitigation projects, and preserving land from development [7]. As a result, New York City was able to avoid the alternative of USD 6 billion in capital costs for large water filtration infrastructure.*

- *Measuring ecosystem services through Gross Ecosystem Product (GEP): China has adopted this metric, which was approved by the UN Statistical Committee in 2021. Studies have calculated GEP of Qinghai in 2015 to be 185.4 billion Yuan, of which water supply contributed more than half of its GEP. This largely because Qinghai is the source of three rivers - the Mekong, Yangtze and Yellow River. Modelling found that about two-third of ecosystem services was exported outside of Qinghai. By measuring the value and location of the production and usage of ecosystem services, GEP provides a basis for financial flows across regions [8].*

- *Valuation of inland waters by the City of Stockholm: The city used a valuation methodology to derive that the total benefits (£230-260m) of reaching good water quality exceeded the cost of measures (£92m) required. This helped Stockholm's Environment and Health Administration to understand the economic value of achieving good water quality in all inland waters of the city [9].*

References

Olam Group, "Strengthening Connections for a Sustainable Future," Olam Group, 2023.

United Utilities, "Corporate Natural Capital Account for United Utilities," United Utilities, 2023.

Pepsico, "Water," [Online]. Available: https://pepsico.com/our-impact/esg-topics-a-z/water.

ODI, "Water management and stewardship: taking stock of corporate water behavior," p. 132.

Schneider Electric, "Changing Tides: The Future of Water-Risk Disclosure Requirements," 23 4 2024. [Online]. Available: https://perspectives.se.com/blog-stream/changing-tides-the-future-of-water-risk-disclosure-requirements.

Natural Capital Valuation: A Tool to Incorporate Nature while Designing Development Projects, [Online]. Available: https://www.aiib.org/en/news-events/media-center/blog/2024/Natural-Capital-Valuation-A-Tool-to-Incorporate-Nature-while-Designing-Development-Projects.html.

The New York Times, "A Billion-Dollar Investment in New York's Water," 2018. [Online].

Z. O. e. al., "Using Gross Ecosystem Product (GEP) to value nature in decision making," *Proceedings of the National Academy of Sciences,* vol. 117, 2020.

Capitals Coalition, "Case Studies," [Online]. Available: https://capitalscoalition.org/impact/case-studies/.